Theoretical Modeling for the STEREO Mission

Markus Aschwanden et al.
Lockheed Martin Solar & Astrophysics Laboratory

Solar-B/STEREO Workshop, Turtle Bay Resort, Oahu, Hawaii – Nov 15-18, 2005

Ref.: Aschwanden et al. (2005), Space Science Rev., (subm.)
http://www.lmsal.com/~aschwand/publications/eprints/2005_stereobook.pdf

et al.:

GSFC: L.F.Burlaga, M.L.Kaiser, C.K.Ng, D.V.Reames, M.J. Reiner

Univ.Michigan: T.I.Gombosi, N.Lugaz, W.IV.Ward Manchester, II.Roussev, T..H.Zurbuchen

Univ.New Hampshire: C.J.Farrugia, A.Galvin, M.A.Lee

SAIC: J.A.Linker, Z.Mikic, P.Riley

Rice Univ: D.Alexander, A.W.Sandman

NRL: J.W.Cook, R.A.Howard

NOAA/SEC: D.Odstrcil, V.Pizzo

JPL: P.C.Liewer, E.DeJong

UCB: J. Luhmann

MPIS: B.Inhester, R.W.Schwenn, S.Solanki, V.M.Vasyliunas, T.Wiegelmann

Univ.Bern: L.Blush, P.Bochsler

Univ.Sydney: I.H.Cairns, P.A.Robinson

Univ.Goettingen: V.Bothmer

KFIK RMKI, Budapest, Hungary: K.Kecskemety

Univ.Arizona: J.Kota

CNRS: A. Llebaria

CNRS, LESIA: Maksimovic

MPES: M.Scholer

Univ. Kiel: R.Wimmer-Schweingruber

Phenomena vs. STEREO Detection

Metrics of modeled solar/heliospheric phenomena versus detecting STEREO instruments.

	SECCHI EUVI, COR/HI	SWAVES	IMPACT[1])	PLASTIC
Background Plasma:				
Solar corona (§2)	EUV,WL	...	...	...
Solar wind (§3)	...	waves	particles	particles
CME Initiation:				
Filament eruption (§4)	EUV,WL	...	...	...
Coronal mass ejection launch (§5)	EUV,WL	radio, waves	...	...
CME Propagation:				
Interplanetary shocks (§6)	WL	radio, waves	particles	particles
Interplanetary particle beams (§7)	...	radio, waves	particles	particles
Solar energetic particle events (§8)	...	...	particles	particles
Geo-connected space weather (§9)	...	...	particles	particles

[1] IMPACT will also be able to make in-situ measurements of the magnetic field at 1 AU.

1. Modeling the Solar Corona

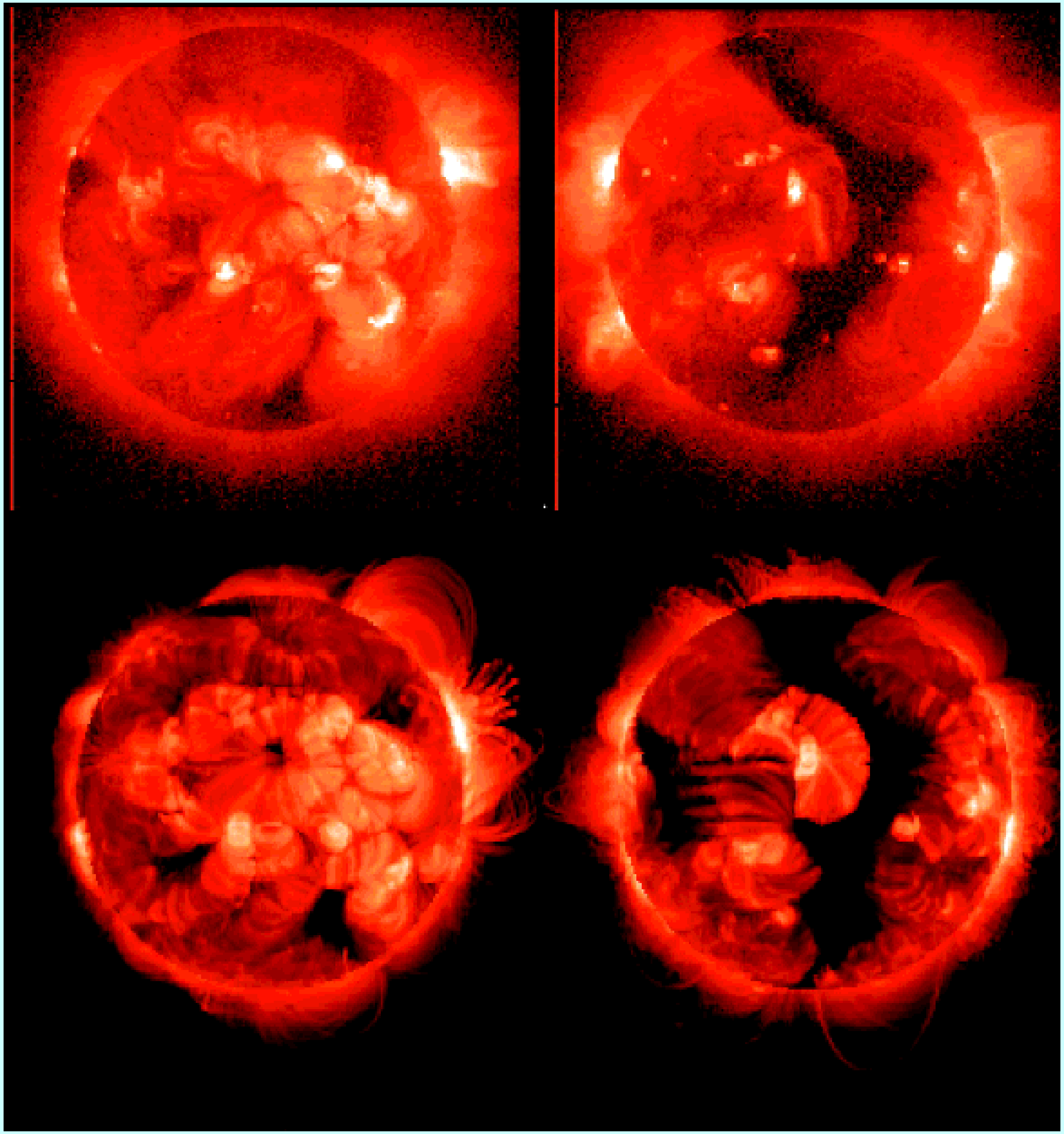

Schrijver, Sandman, Aschwanden, & DeRosa (2004)

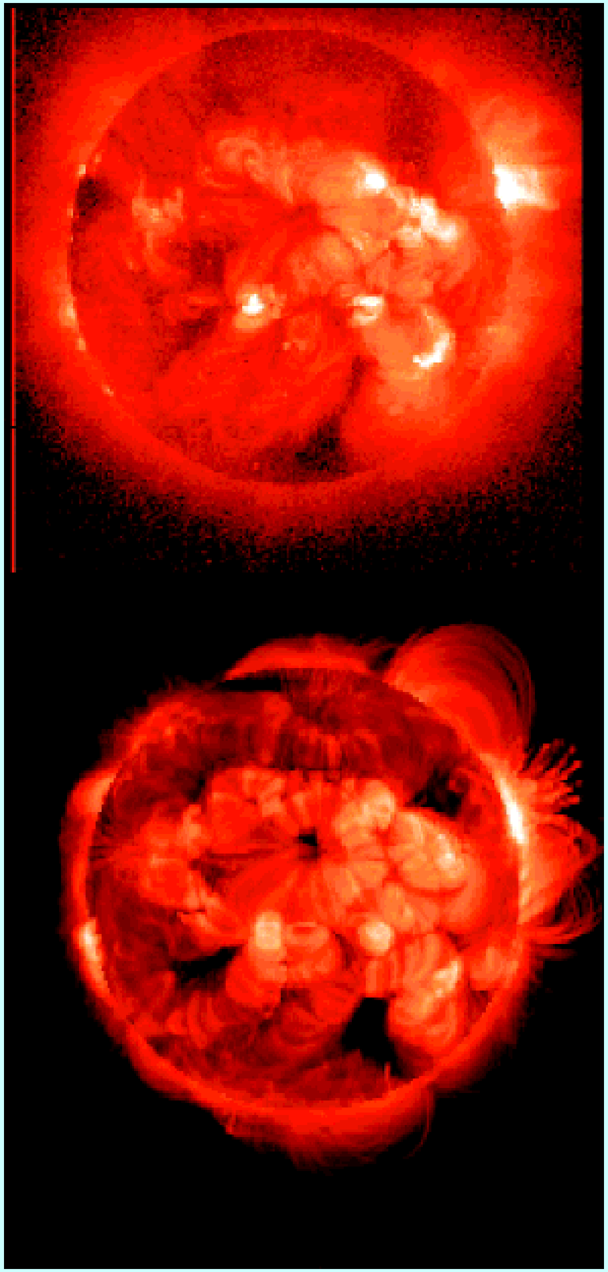

A full-scale 3D model of the solar corona:
(Schrijver et al. 2004)

-3D magnetic field model (using Potential source surface model) computed from synoptic (full-Sun) photospheric magnetogram→10^5 loop structures

-Coronal heating function

$$E_H(x,y,z=0) \sim B(x,y)^a * L(x,y)^b \qquad a \sim 1,\ b \sim -1$$

-Hydrostatic loop solutions

$$E_H(s)-E_{rad}(s)-E_{cond}(s)=0$$

yield density $n_e(s)$ and $T_e(s)$ profiles

-Line-of-sight integration yields DEM for every image pixel

$$dEM(T,x,y)/ds = \int n_e^2(x,y,z,T[x,y,z])\, dz$$

-Free parameters can be varied until synthetic image matches observed ones in each temperature filter

-STEREO will provide double constraint with two independent line-of-sights.

Hydrostatic/hydrodynamic modeling of coronal loops requires careful disentangling of neighbored loops, background modeling, multi-component modeling, and multi-filter temperature modeling. Accurate modeling requires the identification of elementary loops.

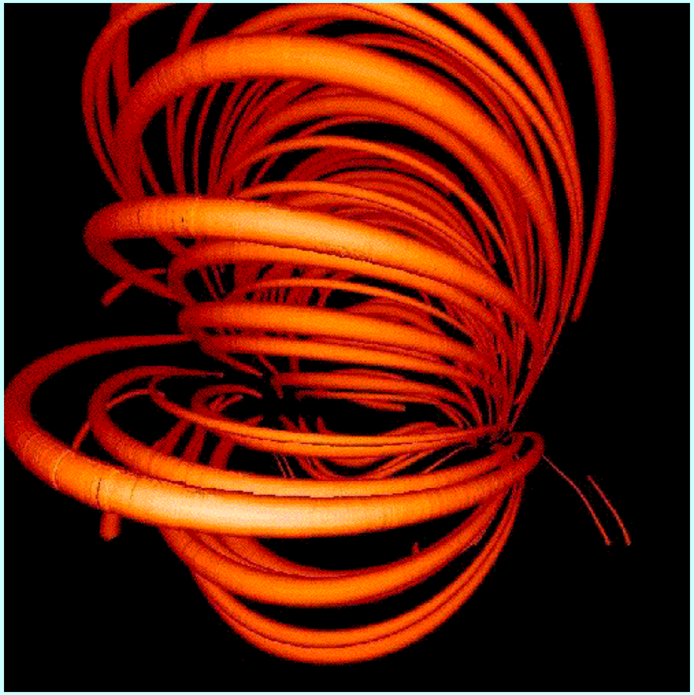

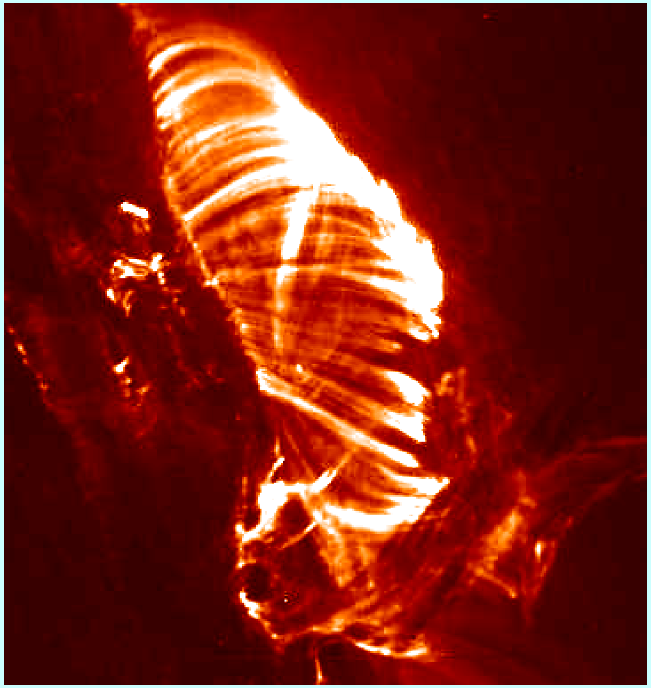

<u>Inversion of coronal density</u> with coarse Resolution (~15 heliographic deg):

-<u>White light inversion</u> (Thomson scattering)

Van de Hulst (1950)

Lamy et al. (1997)

Llebaria et al. (1999)

-<u>Soft X-ray tomography</u>

Hurlburt et al. (1994)

Davila (1994)

Zidowitz (1997)

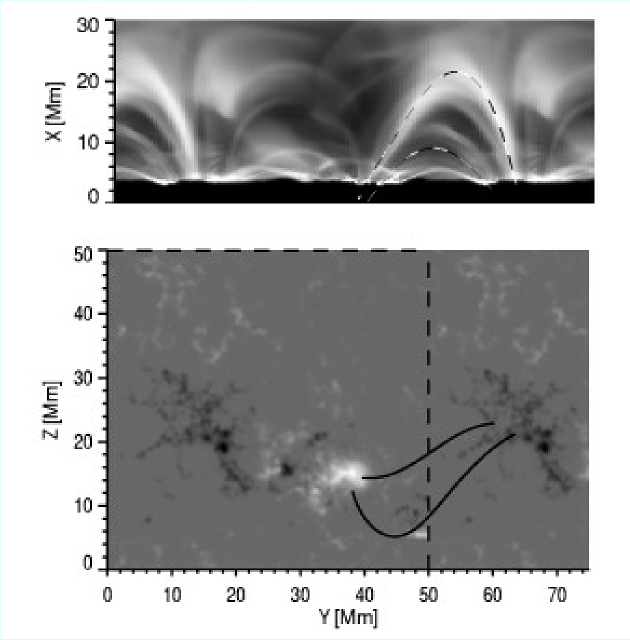

<u>Numerical MHD simulations (~1" pixels):</u>

Gudiksen & Nordlund (2002, 2005)

Mok et al. (2005)

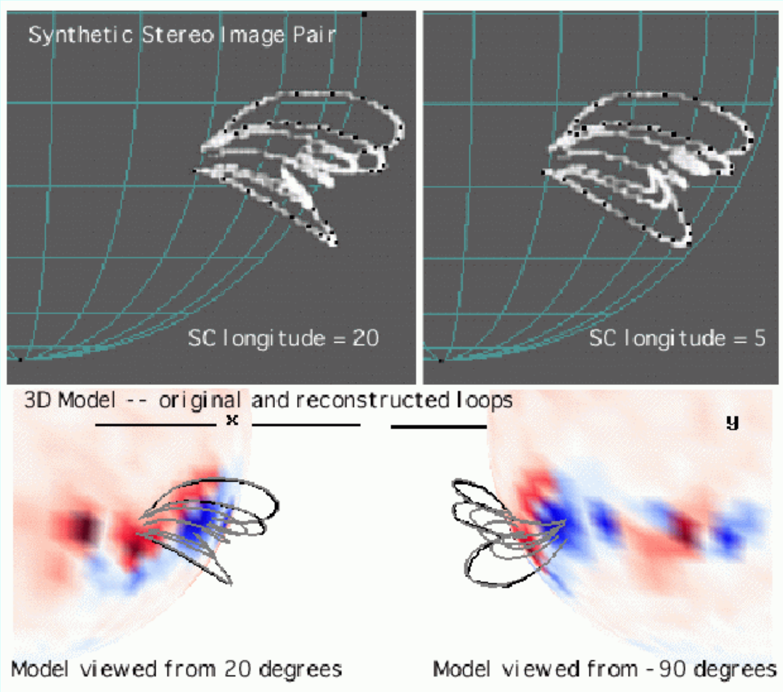

Stereoscopic reconstruction of coronal loops, 3D-geometry:

- -Loughhead, Wang & Blows (1983
- -Berton & Sakurai (1985)

Tie-point method:

- -Liewer et al. (2000)
- -Hall et al. (2004)

Solar-rotation stereoscopy:

- -Koutchmy & Molodensky (1992)
- -Vedenov et al. (2000)

Dynamic stereoscopy:

- -Aschwanden et al. (1999, 2000)

Magnetic field-aided reconstruction:

- -Gary & Alexander (1999)
- -Wiegelmann & Neukirch (2002)
- -Wiegelmann & Inhester (2003)
- -Wiegelmann et al. (2005)

3D-reconstruction of coronal loop structures to test theoretical models of magnetic field extrapolations.

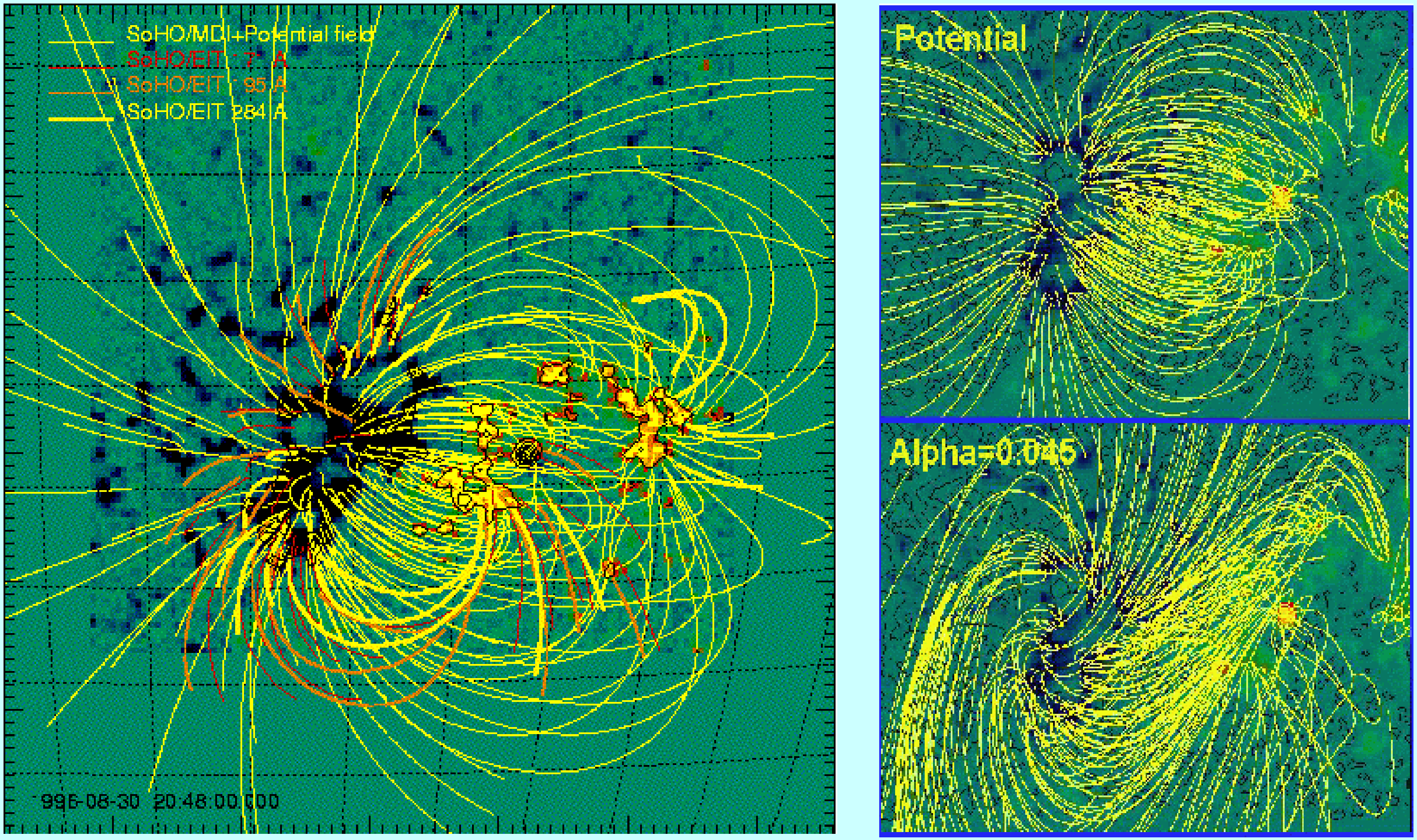

Fingerprinting (automated detection) of curvi-linear structures

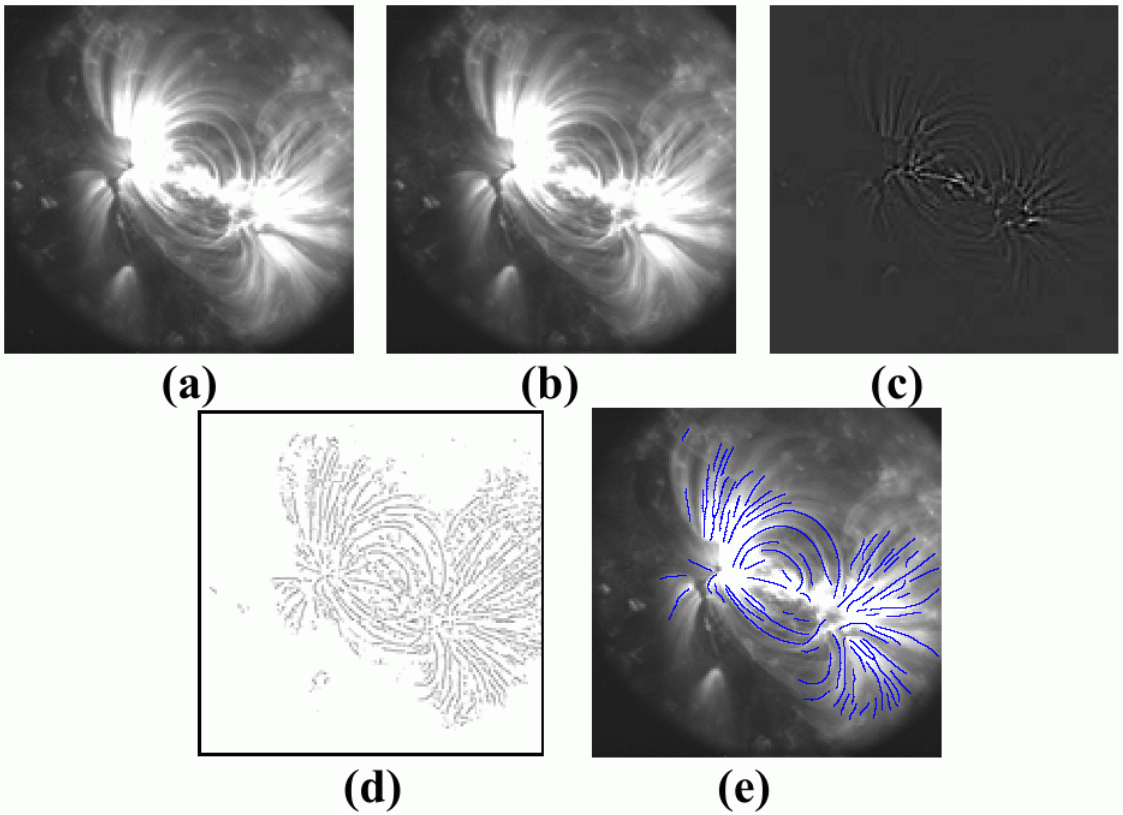

Fig. 1. (a) Coronal image, (b) Median filtered image, (c) Contrast enhanced version of unsharp masked image, (d) Curve features after threshholdings (e) Detected loops.

Lee, Newman & Gary improve detection of coronal loops with "Oriented connectivity Method" (OCM):

-median filtering

-contrast enhancement

-unsharp mask

-detection threshold

-directional connectivity

Lee, Newman, & Gary (2004), 17th Internat. Conf. On Pattern Recognition, Cambridge UK, 23-26 Aug 2004

Elementary vs. Composite loops:

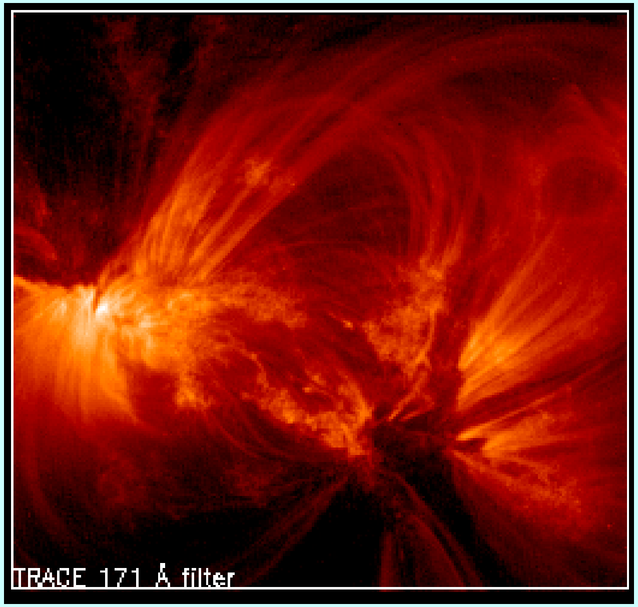

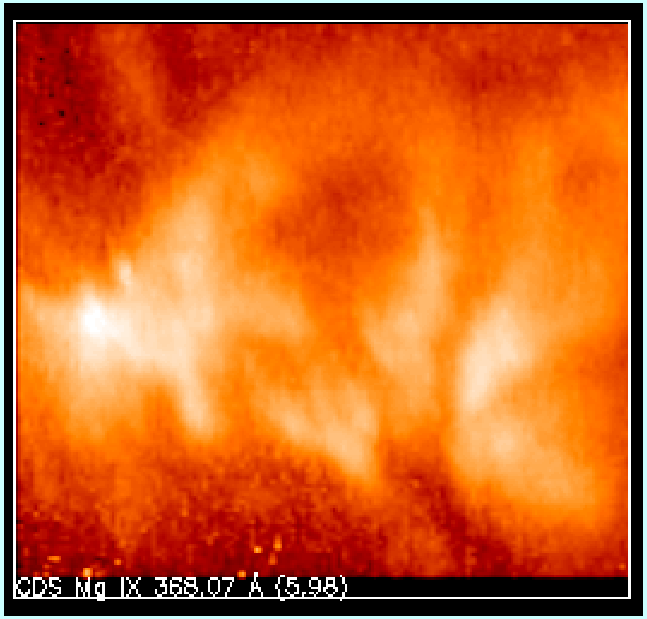

Each loop strand represents an "isolated mini-atmosphere" and has its own hydrodynamic structure T(s), n_e(s), which needs to be extracted by subtracting it from the background coronal structures.

→SECCHI/EUVI (1.6" pixels) will be able to resolve some individual loops, substantially better than CDS (4" pixels), but somewhat less than TRACE (0.5" pixels).

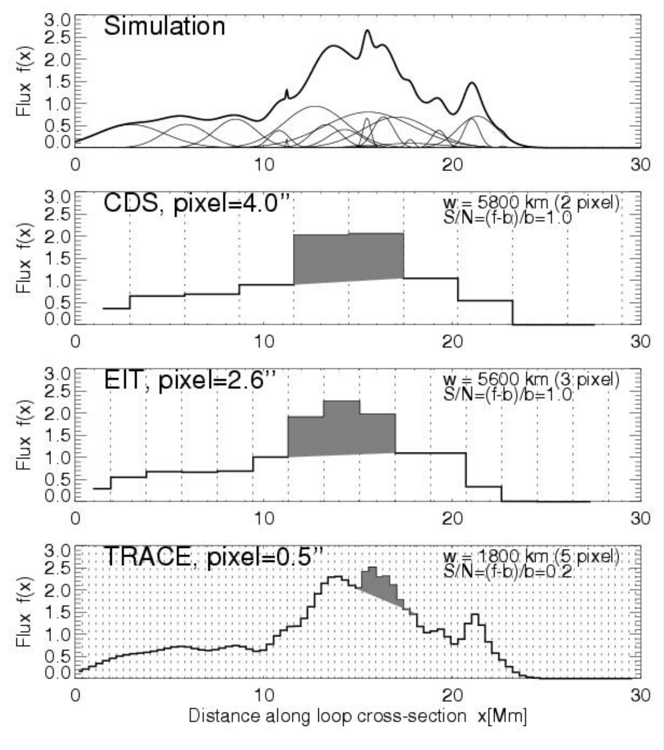

Loops	Widths	Loop/Backgr.	Instrument	Ref.
1	~12 Mm	?	CDS	Schmelz et al. (2001)
10	?	170%±150%	EIT	Schmelz et al. (2003)
30	7.1±0.8 Mm	30%±20%	EIT	Aschwanden et al. (1999)
1	~5.8 Mm	76%±34%	TRACE/CDS	DelZanna & Mason (2003)
41	3.7±1.5 Mm	?	TRACE	Aschwanden et al. (2000) (no highpass filter)
234	1.4±0.2 Mm	8%±3%	TRACE	Aschwanden & Nightingale 2005 (with highpass filter)

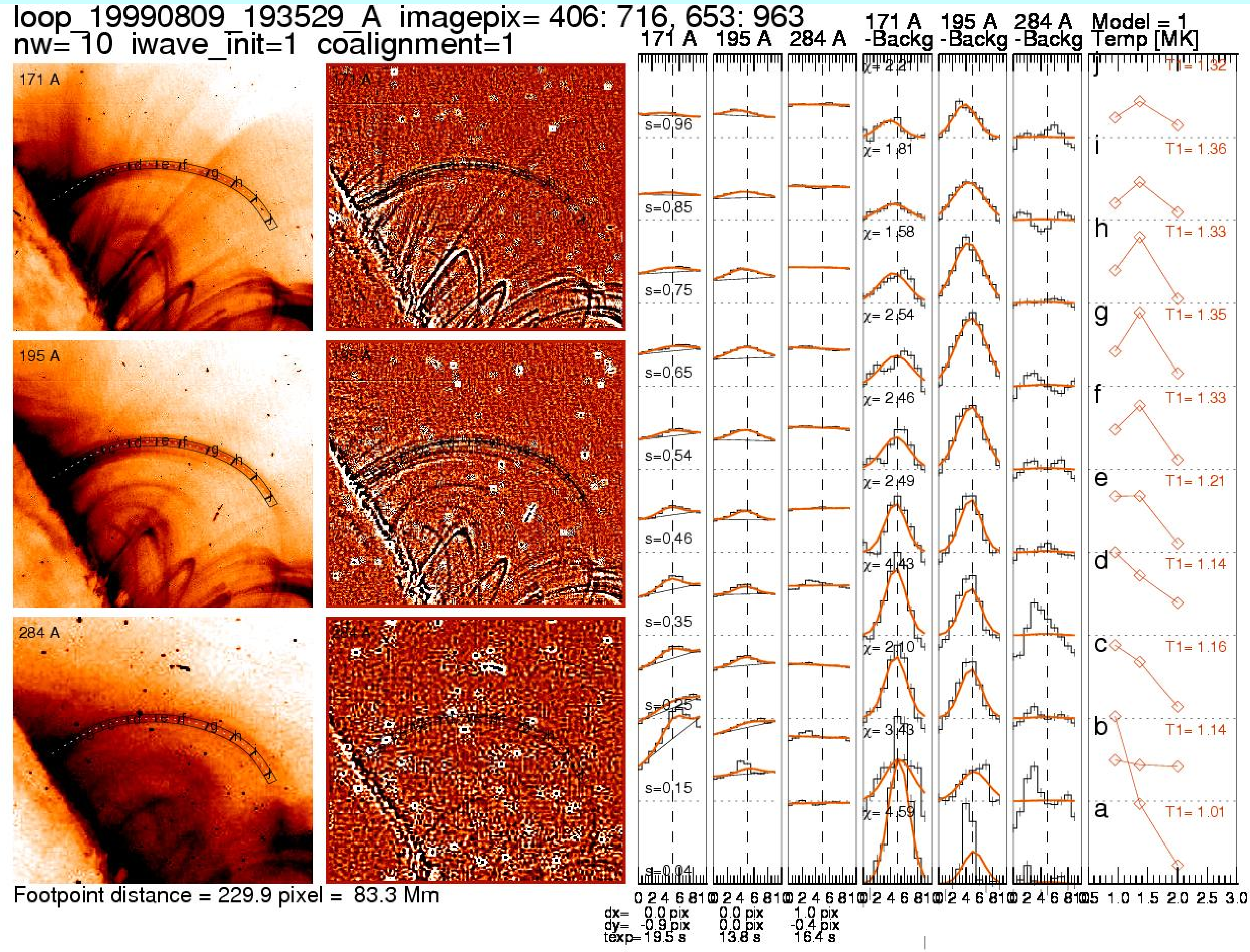

loop_19990809_193529_A imagepix= 406: 716, 653: 963
nw= 10 iwave_init=1 coalignment=1
171 A
195 A
284 A
171 A -Backg
195 A -Backg
284 A -Backg
Model = 1
Temp [MK]
s=0.96
s=0.85
s=0.75
s=0.65
s=0.54
s=0.46
s=0.35
s=0.25
s=0.15
s=0.04
χ= 2.21
χ= 1.81
χ= 1.58
χ= 2.54
χ= 2.46
χ= 2.49
χ= 4.43
χ= 2.10
χ= 3.43
χ= 4.59
j T1= 1.32
i T1= 1.36
h T1= 1.33
g T1= 1.35
f T1= 1.33
e T1= 1.21
d T1= 1.14
c T1= 1.16
b T1= 1.14
a T1= 1.01
Footpoint distance = 229.9 pixel = 83.3 Mm
dx= 0.0 pix 0.0 pix 1.0 pix
dy= -0.9 pix 0.0 pix -0.4 pix
texp= 19.5 s 13.8 s 16.4 s

39A

Model:

Forward-
Fitting
to 3 filters
varying T

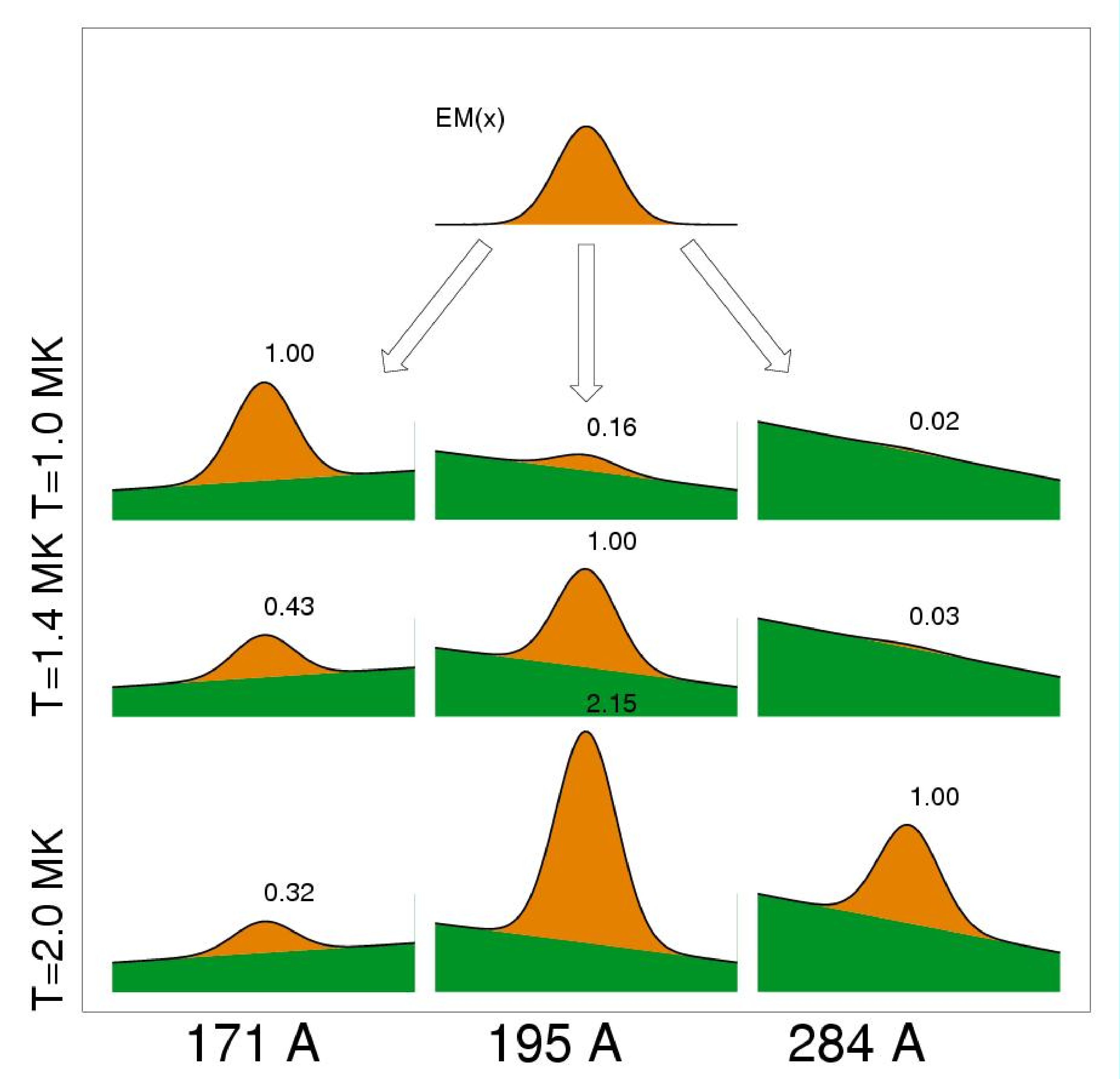

Elementary Loop Strands

The latest TRACE study has shown the existence of elementary loop strands with isothermal cross-sections, at FWHM widths of <2000 km. TRACE has a pixel size of 0.5" and a point-spread function of 1.25" (900 km) and is able to resolve them, while EUVI (1.6" pixels, PSF~3.2"=2300 km) will marginally resolve the largest ones. Triple-filter analysis (171, 195, 284) is a necessity to identify these elementary loop strands.

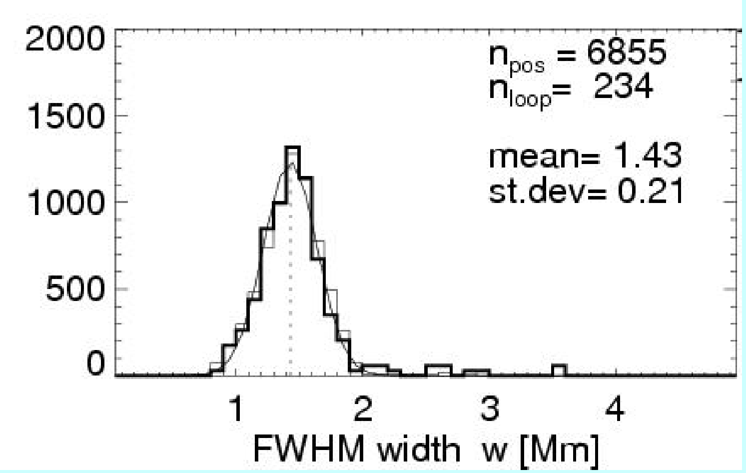

Aschwanden & Nightingale (2005), ApJ 633 (Nov issue)

The advantage of STEREO is that a loop can be mapped from two different directions, which allows for two independent background subtractions. This provides an important consistency test of the loop identity and the accuracy of the background flux subtraction.

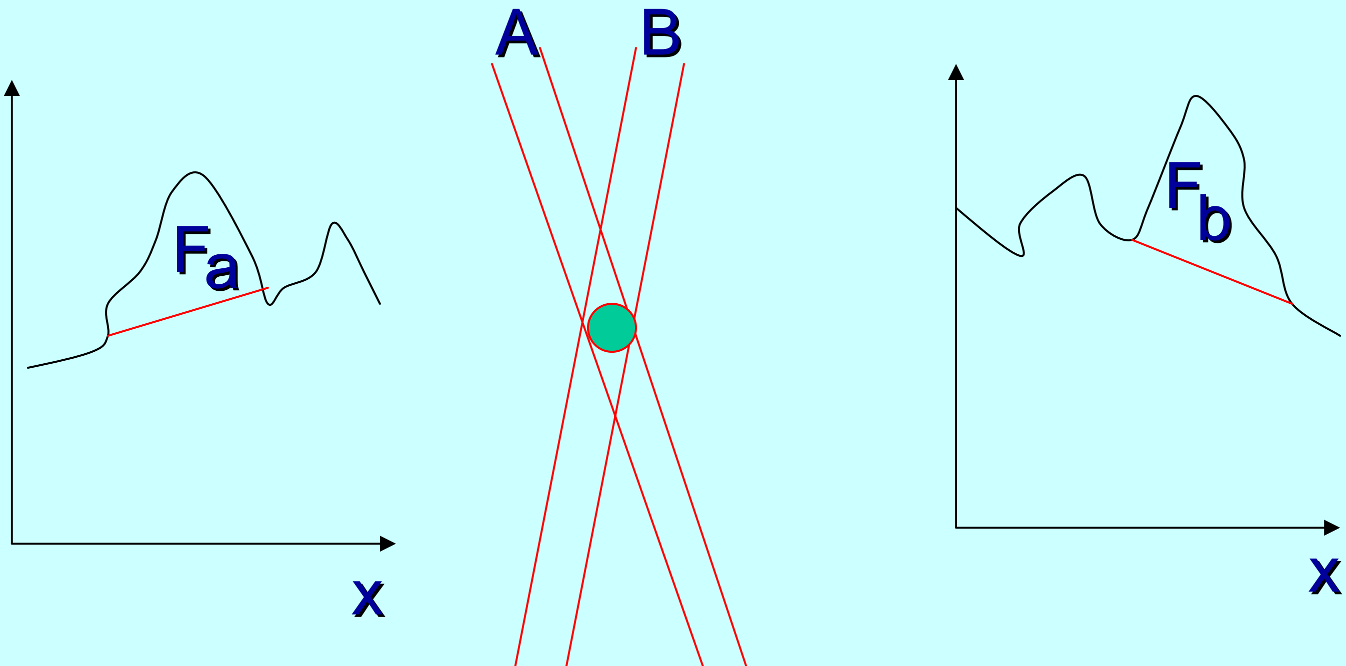

Consistency check: Is F_a = F_b ?

2. Modeling the Solar Wind

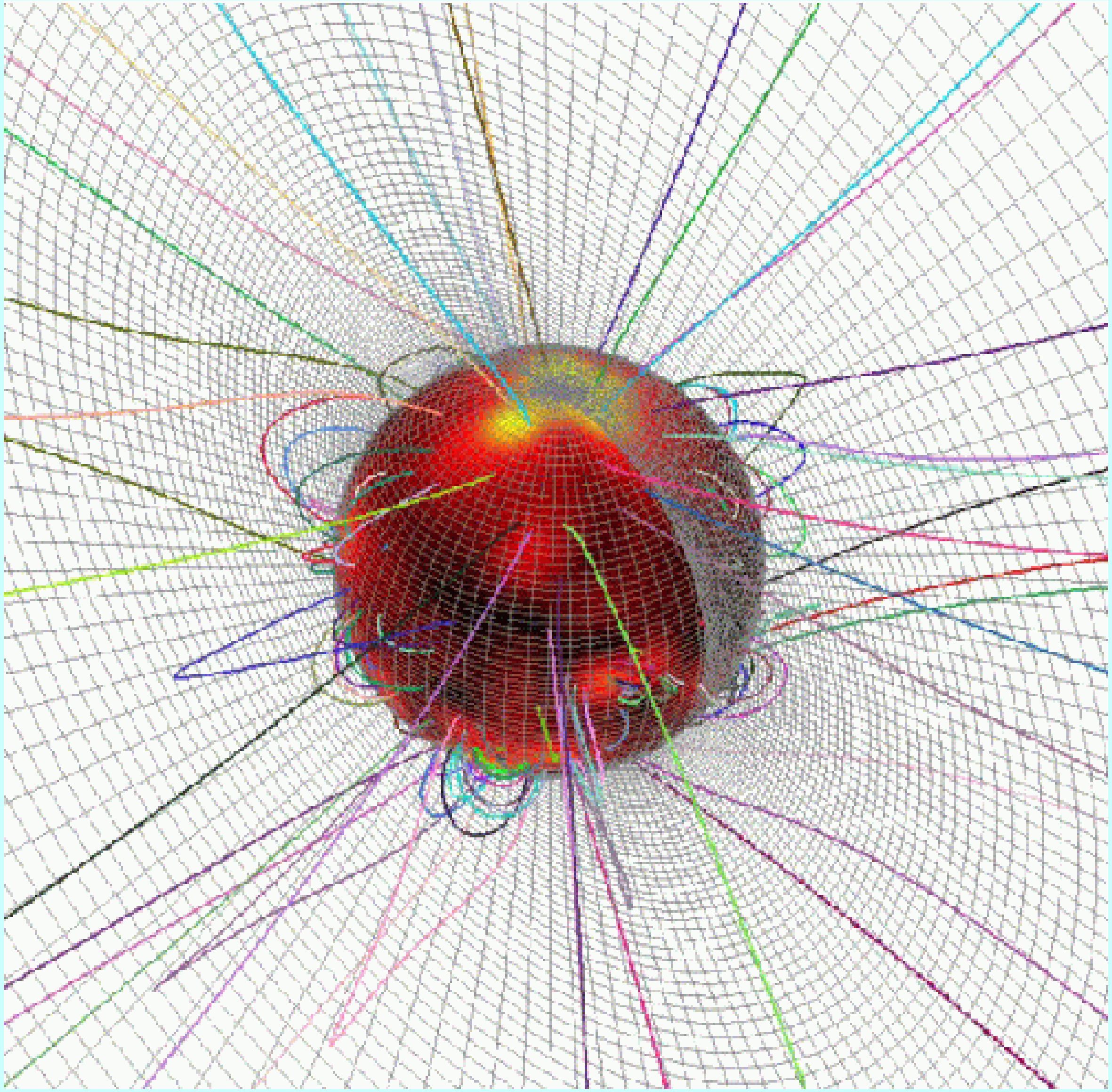

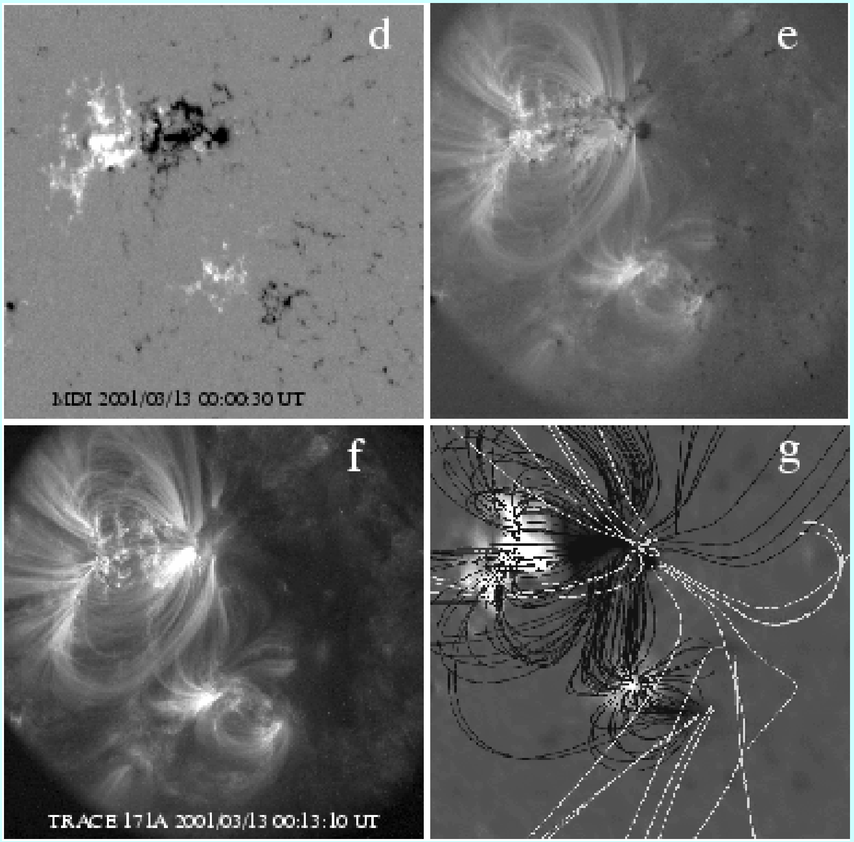

Schrijver & DeRosa (2003)

PFSS-models (Potential Field Source Surface) are used to compute full-Sun 3D magnetic field (current-free $\nabla \times B=0$)

Open fields occur not only in coronal holes, but also in active regions → escape paths of energized particles into interplanetary space

Schrijver & DeRosa (2003) find that ~20%-50% (solar min/max) of interplanetary field lines map back to active regions.

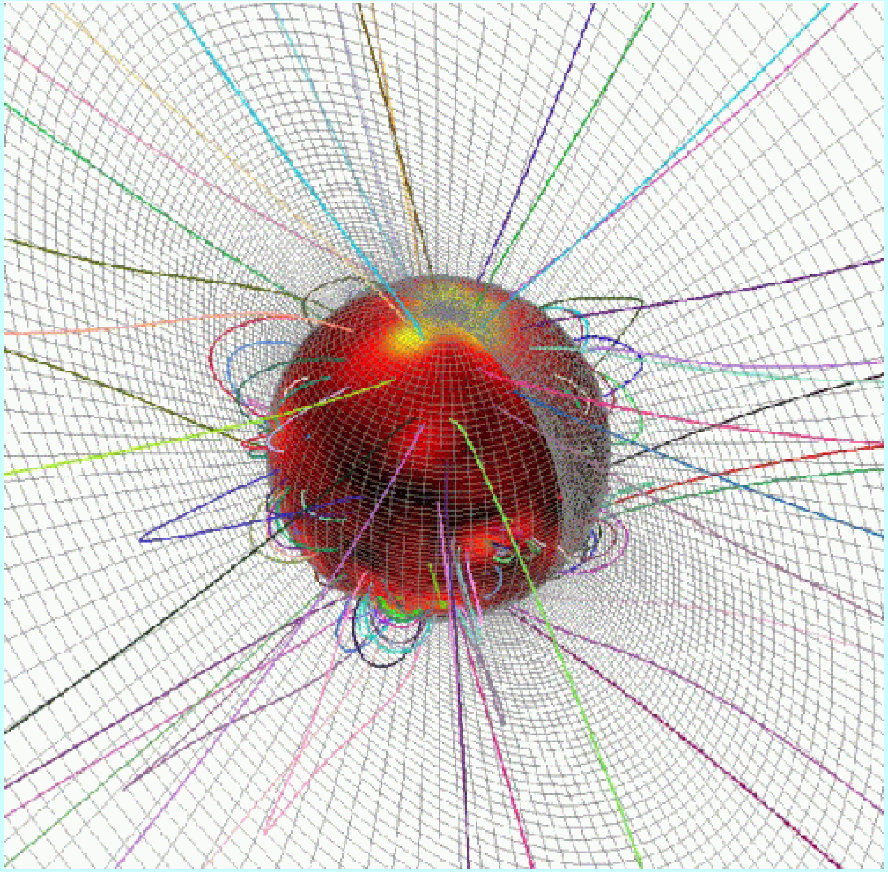

SAIC Magnetohydrodymanics Around a Sphere (MAS)-code models magnetic field B(x,y,z) solar wind speeds v(x,y,z) in range of 1-30 solar radii from synoptic magnetogram

Model computes stationary solution of resistive MHD Equations → n_e, T_e, p, B

MAS model simulates coronal streamers (Linker, vanHoven, Schnack1990)

Line-of-sight integration yields white-light images for SECCHI/ COR and HI

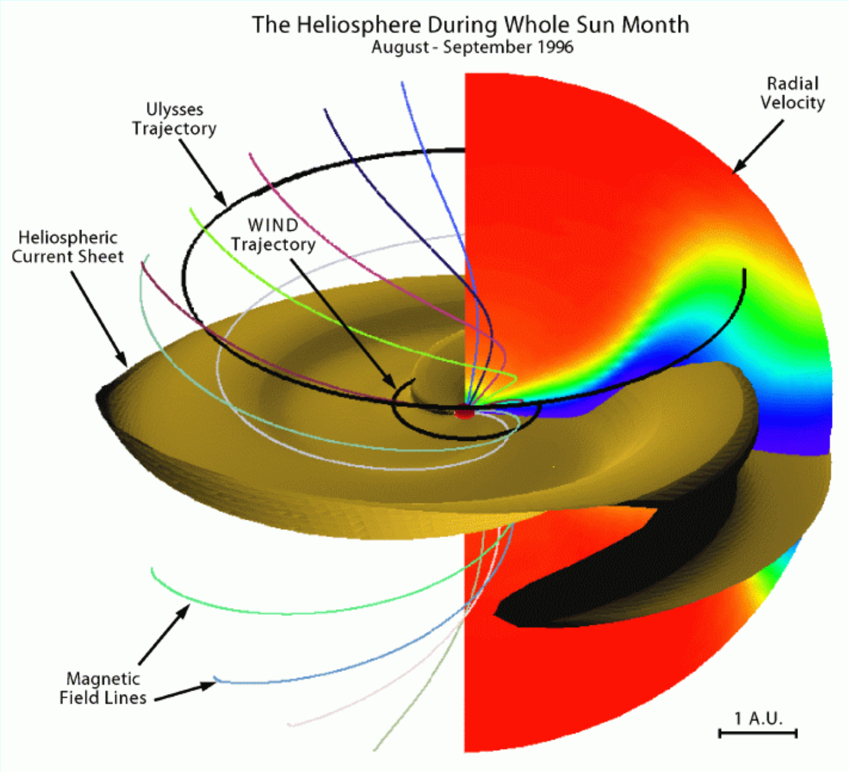

SAIC/MAS-IP code combines corona (1-30 solar radii) and Inner heliosphere (30 Rs -5 AU)

Model reproduces heliospheric current sheet, speeds of fast & slow solar wind, and interplanetary magnetic field

NOAA/ENLIL code (Odstrcil et Al. 2002) is time-dependent 3D MHD code (flux-corrected transport algorithm): inner boundary is sonic point (21.5-30 Rs from WSA code, outer boundary is 1-10 AU.

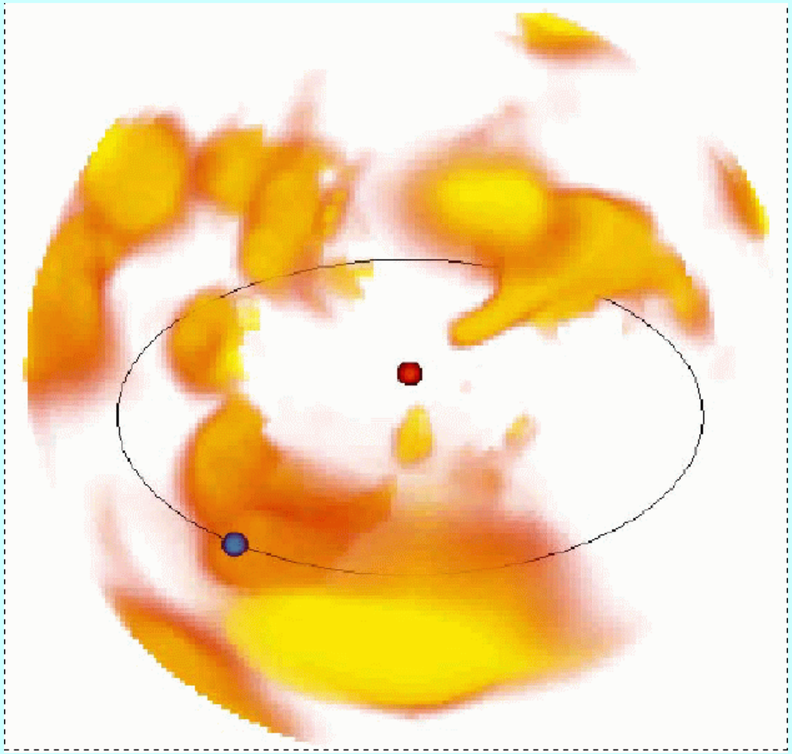

SMEI heliospheric tomography model uses interplanetary scintillation (IPS) data for reconstruction of solar wind (Jackson & Hick 2002)

Exospheric solar wind model computes proton and electron Densities in coronal holes In range of 2-30 Rs (Lamy et al. 2003)

Univ.Michigan solar wind code models solar wind with a sum of potential and nonpotential Magnetic field components (Roussev et al. 2003)

3. Modeling of Erupting Filaments

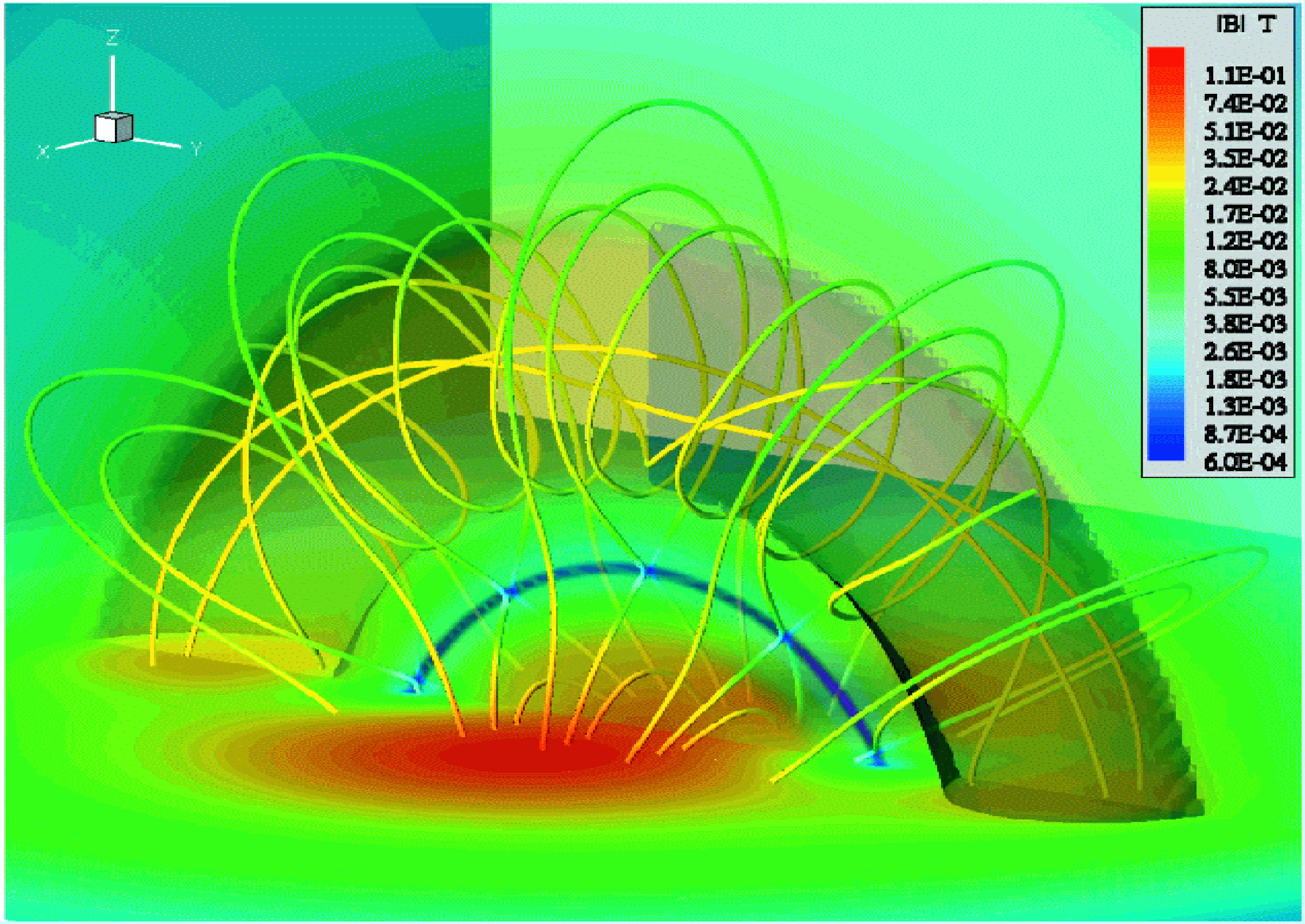

Roussev et al. (2003)

Pre-eruption conditions of filaments

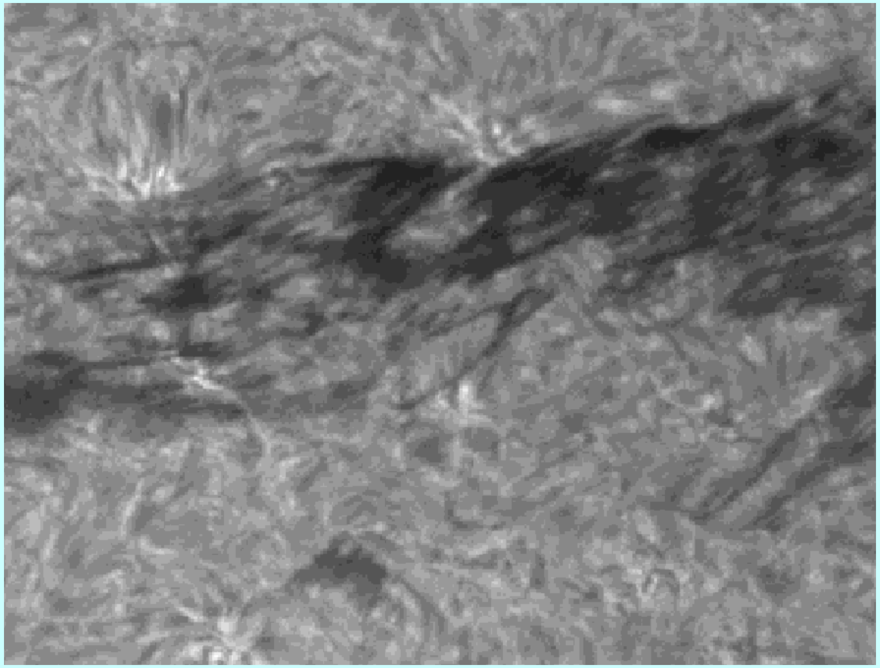

Envold (2001)

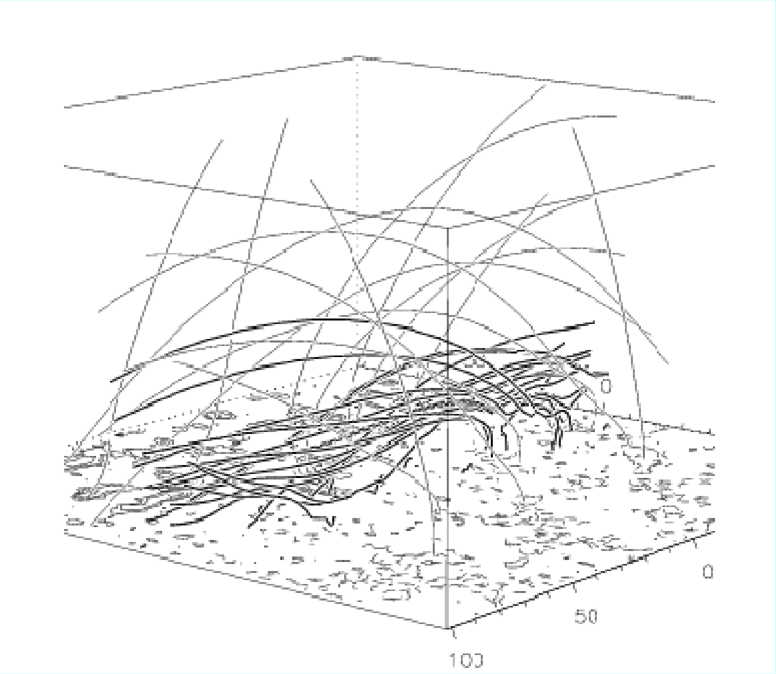

Aulanier & Schmieder (2002)

-Geometry and multi-threat structure of filaments
(helicity, chirality, handedness → conservation, fluxropes)
-Spatio-temporal evolution and hydrodynamic balance
-Stability conditions for quiescent filaments
-Hydrodynamic instability and magnetic instability
of erupting filaments leading to flares and CMEs

Measuring the twist of magnetic field lines

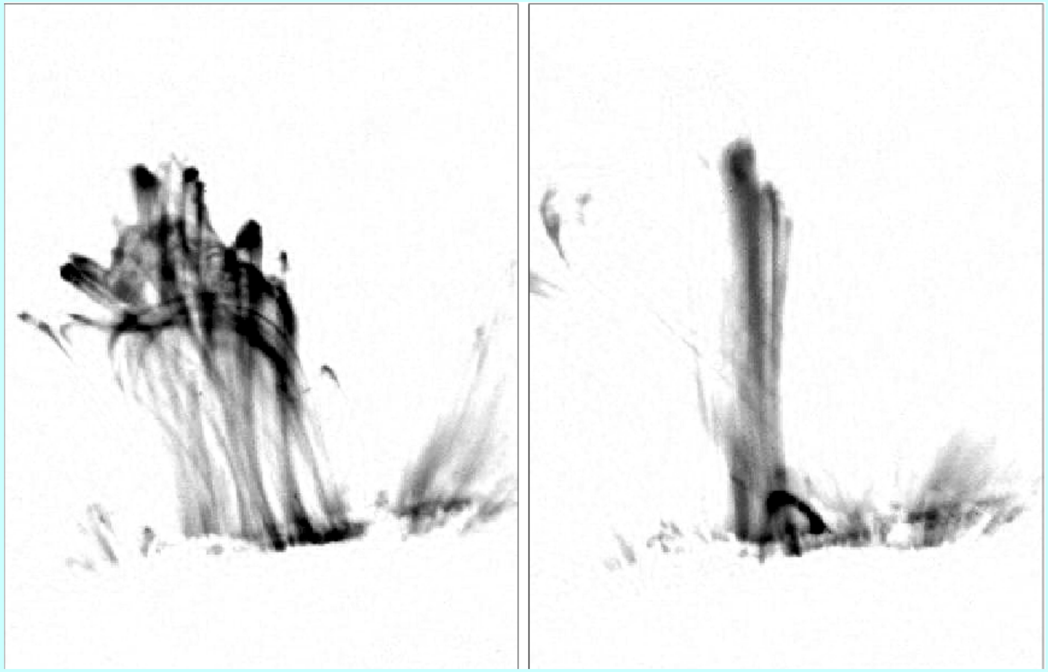

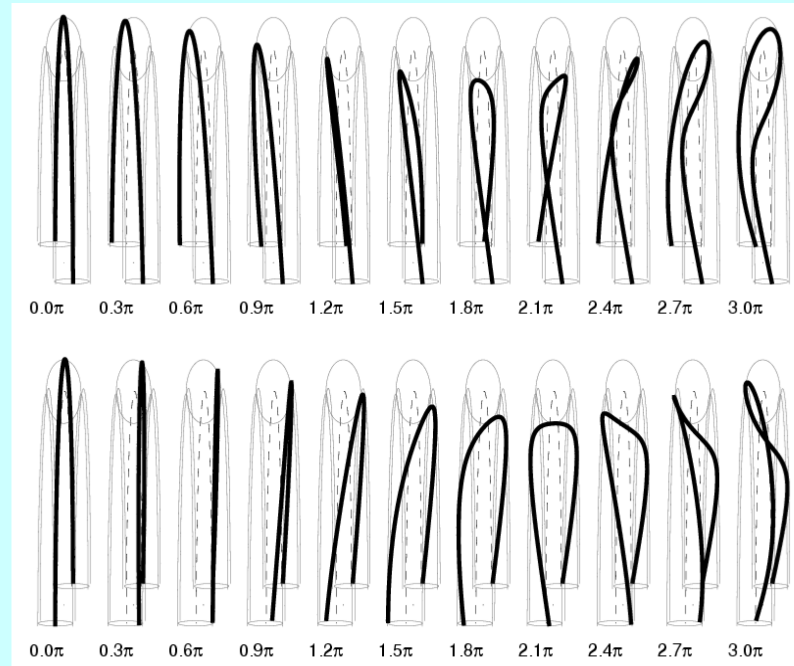

Aschwanden (2004)

-Measuring the number of turns in twisted loops
-Testing the kink-instability criterion for stable/erupting loops
-Monitoring the evolution of magnetic relaxation (untwisting) between preflare and postflare loops

Measuring the twist of magnetic field lines

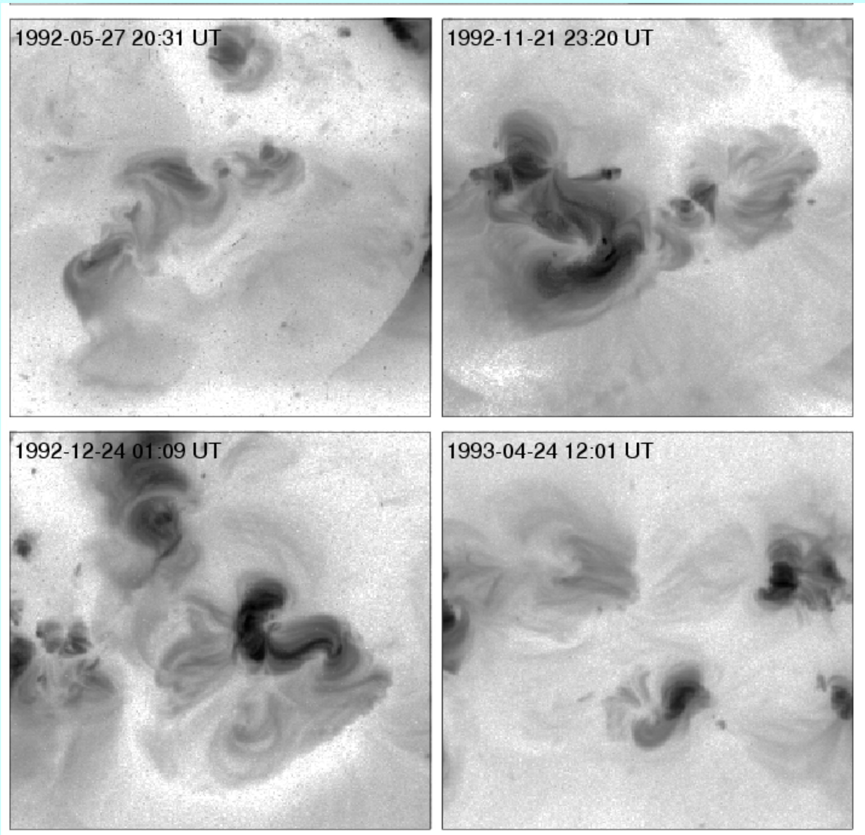

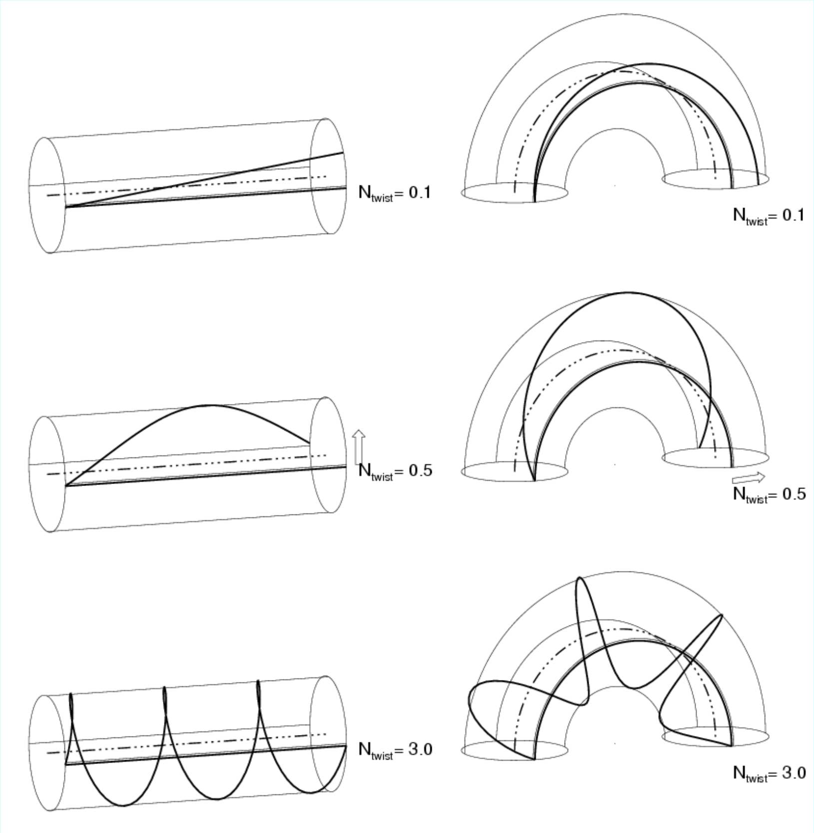

Aschwanden (2004)

-Measuring number of turns in (twisted) sigmoids
before and after eruption

-Test of kink-instability criterion as trigger of flares/CMEs

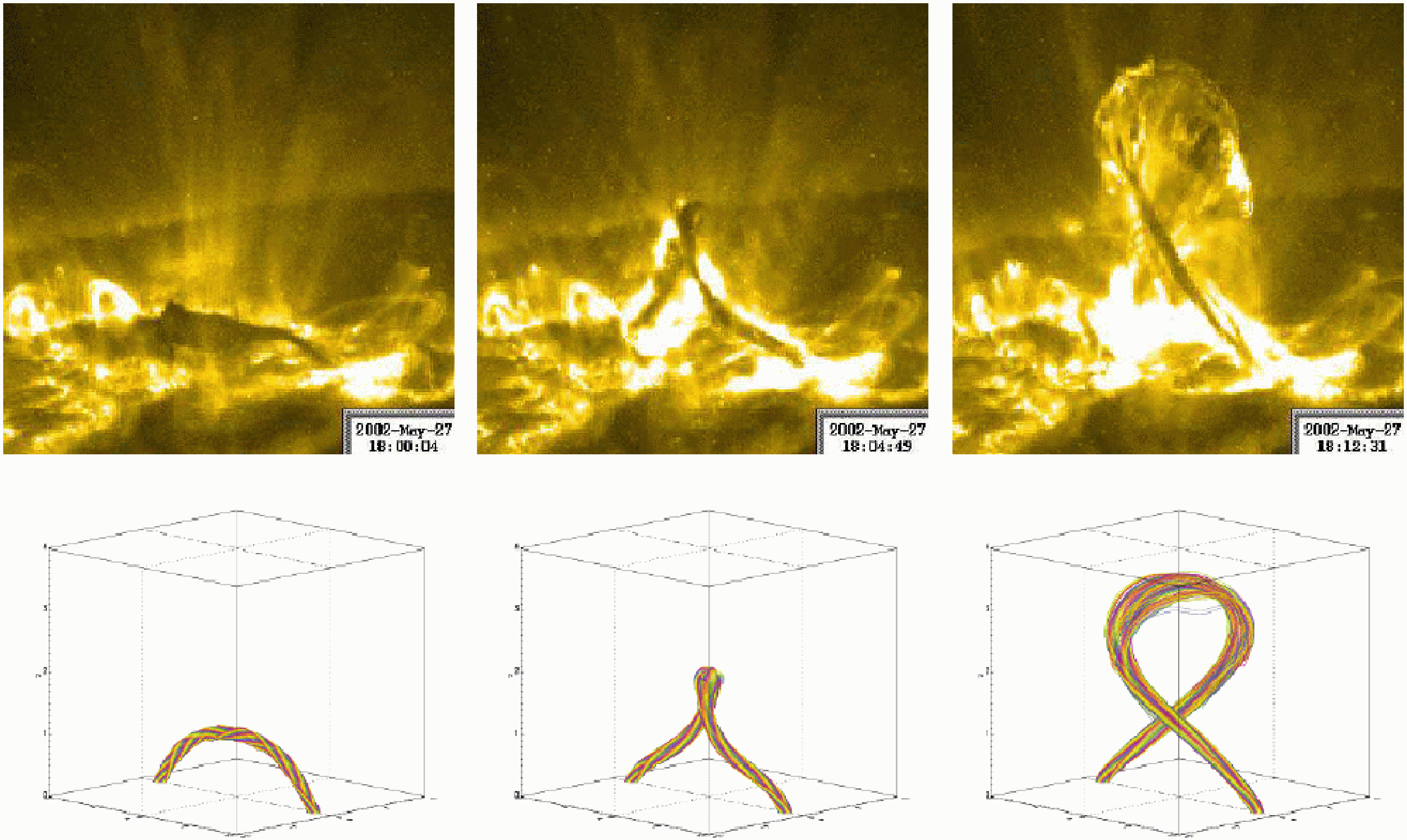

Figure 9. **Top:** TRACE 195 Å images of the confined filament eruption on 2002 May 27. The right image shows the filament after it has reached its maximum height. **Bottom:** magnetic field lines outlining the kink-unstable flux rope reproduced with 3D MHD simulations (Török & Kliem 2004).

Measuring the twist of erupting fluxropes

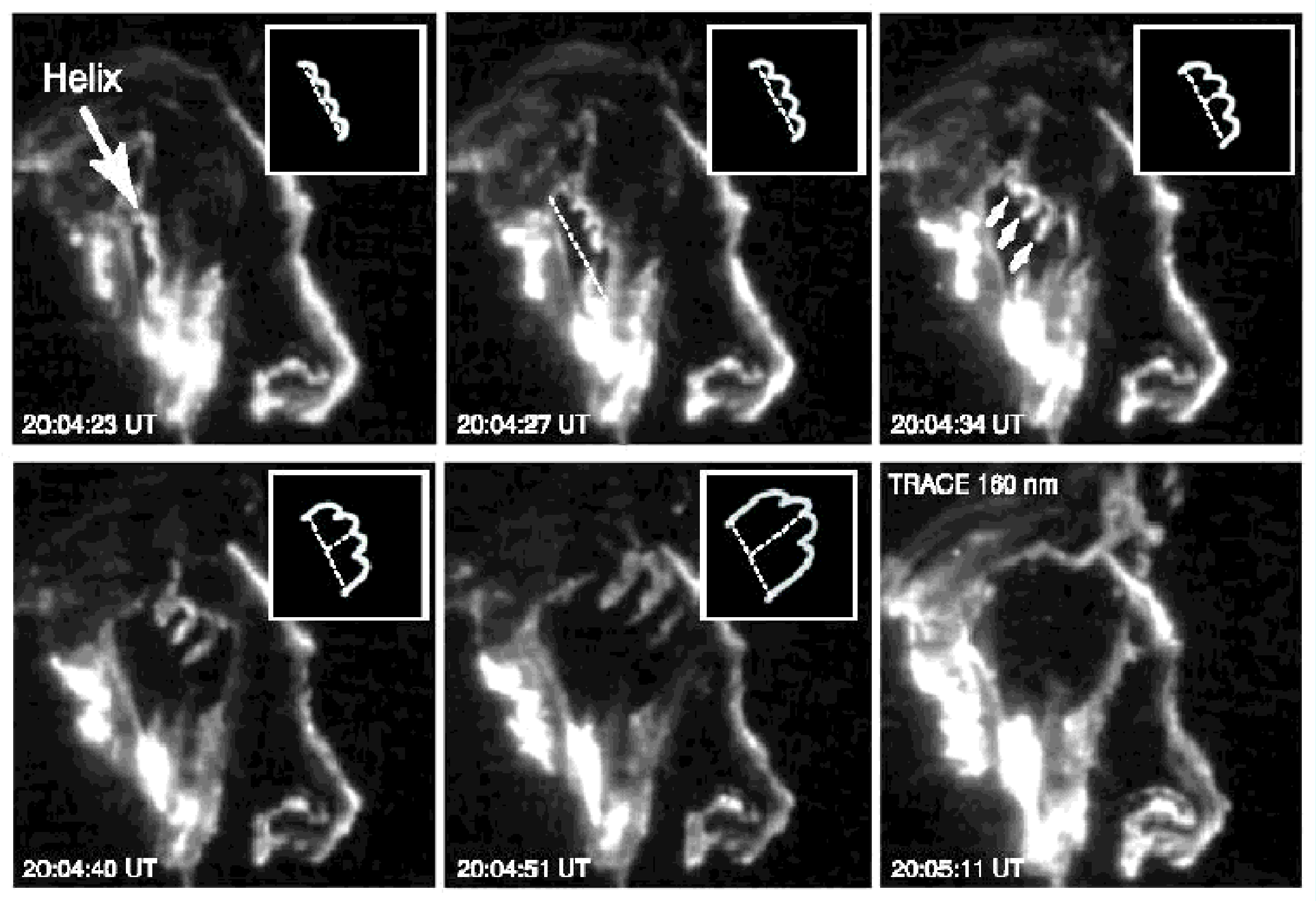

Gary & Moore (2004)

-Measuring number of turns in erupting fluxropes

-Test of kink-instability criterion as trigger of flares/CMEs

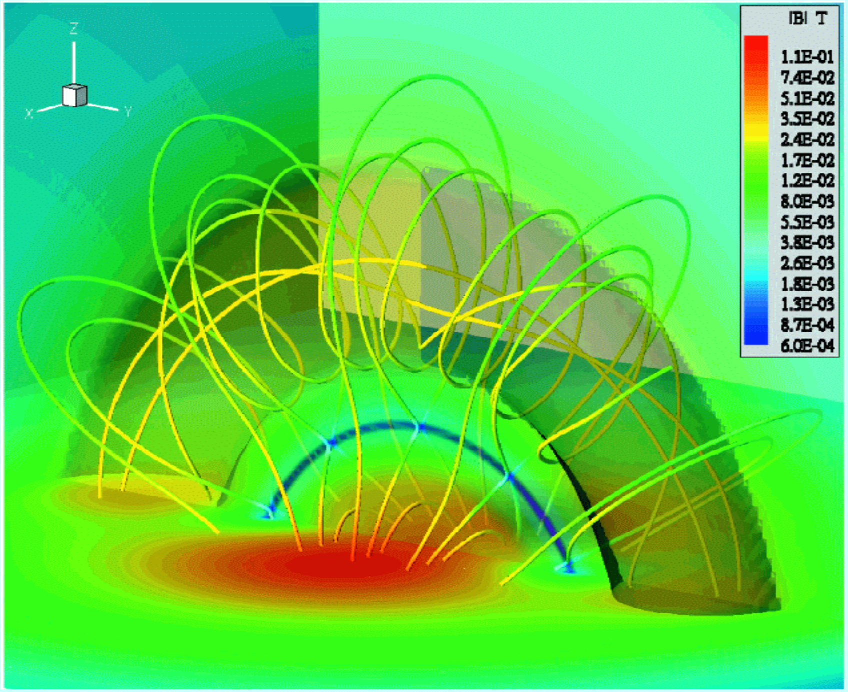

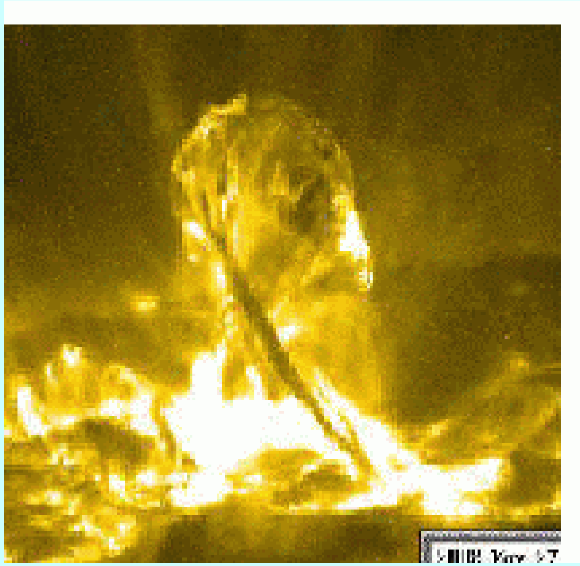

Triggers for of filaments or
Magnetic flux ropes:

-draining of prominence material
→bouancy force
(Gibson & Low 1998)
(Manchester et al. 2004)

-current increase and
loss of equilibrium
(Titov & Demoulin 1999)
(Roussev, Sokolov, & Forbes)
(Roussev et al. 2003)

-kink instability
→ unstable if twist > 3.5π
(Toeroek & Kliem 2003,
Toeroek, Kliem, & Titov 2003)

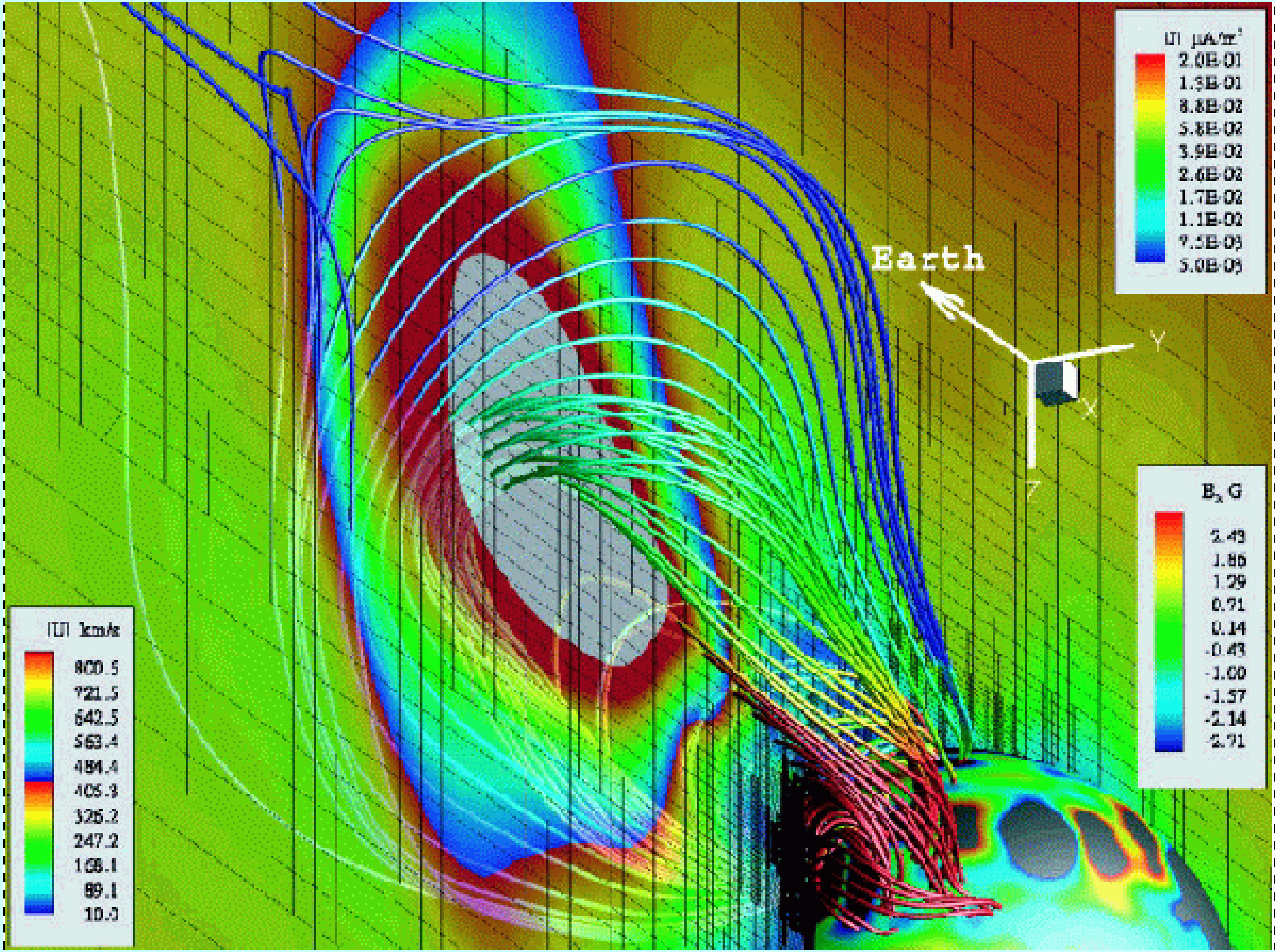

Roussev et al. (2004)

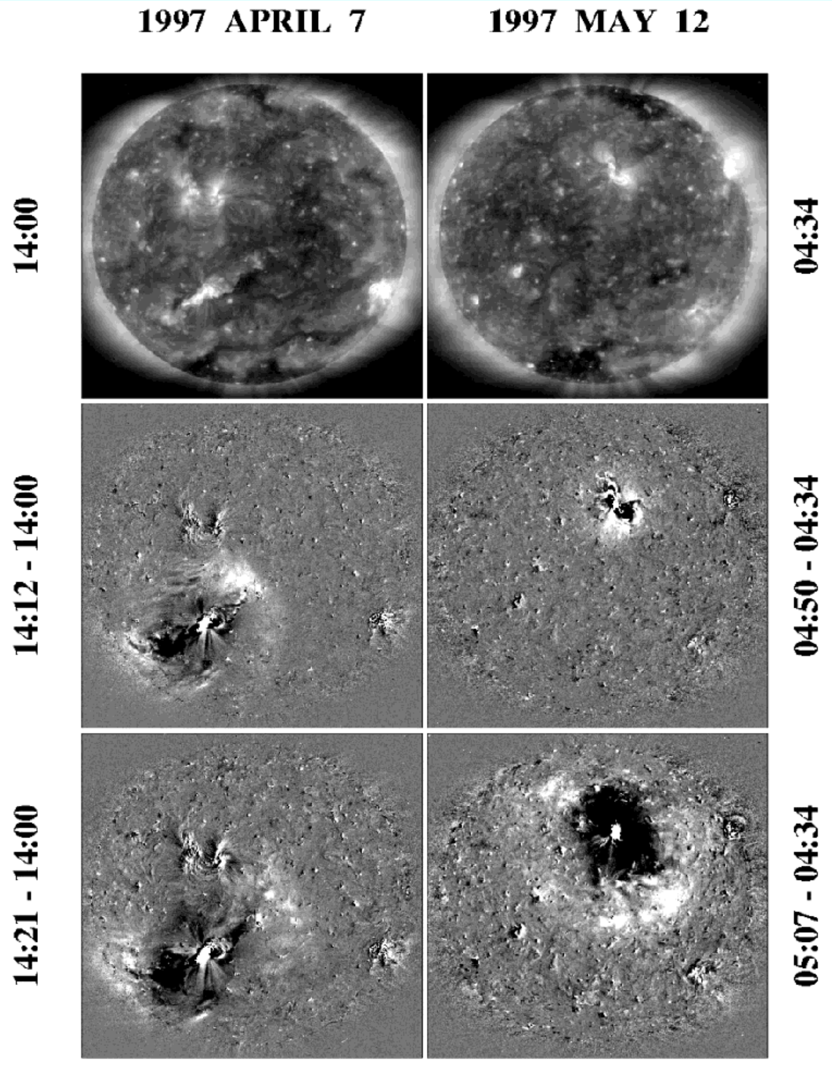

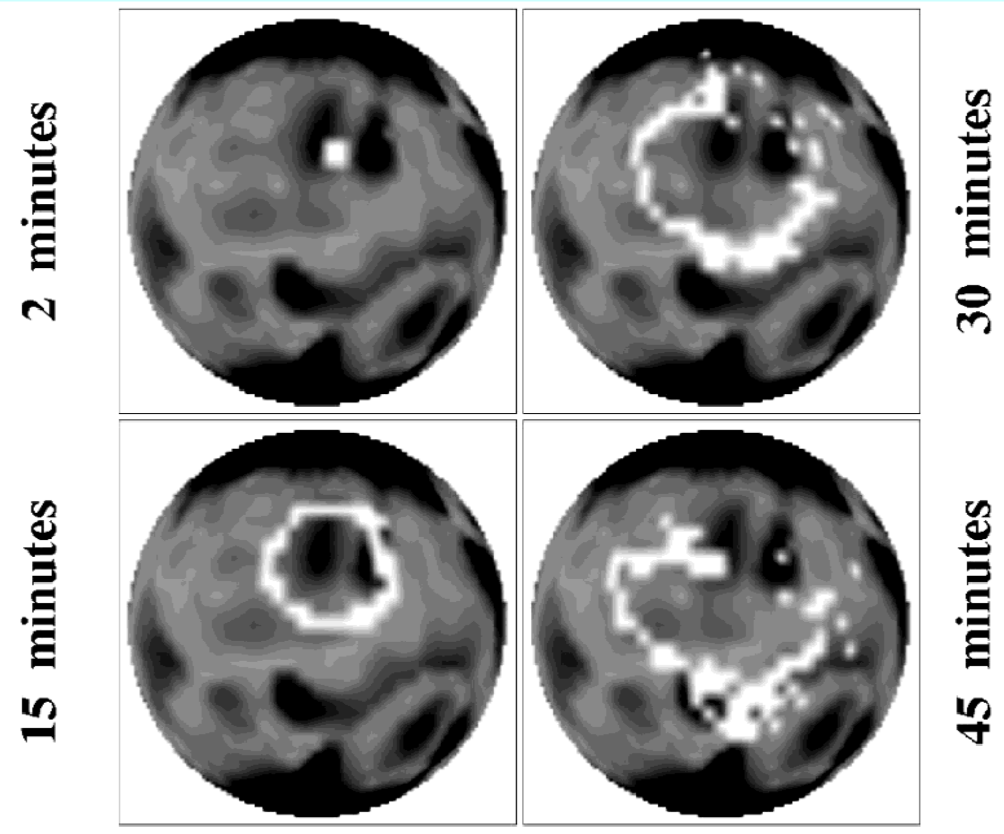

<u>MHD simulations of coronal dimming:</u>

-evacuation of plasma beneath CME, fast-mode MHD wave (Wang 2000; Chen et al. 2002; Wu et al. 2001)

5. Modeling of Coronal Mass Ejections (CMEs)

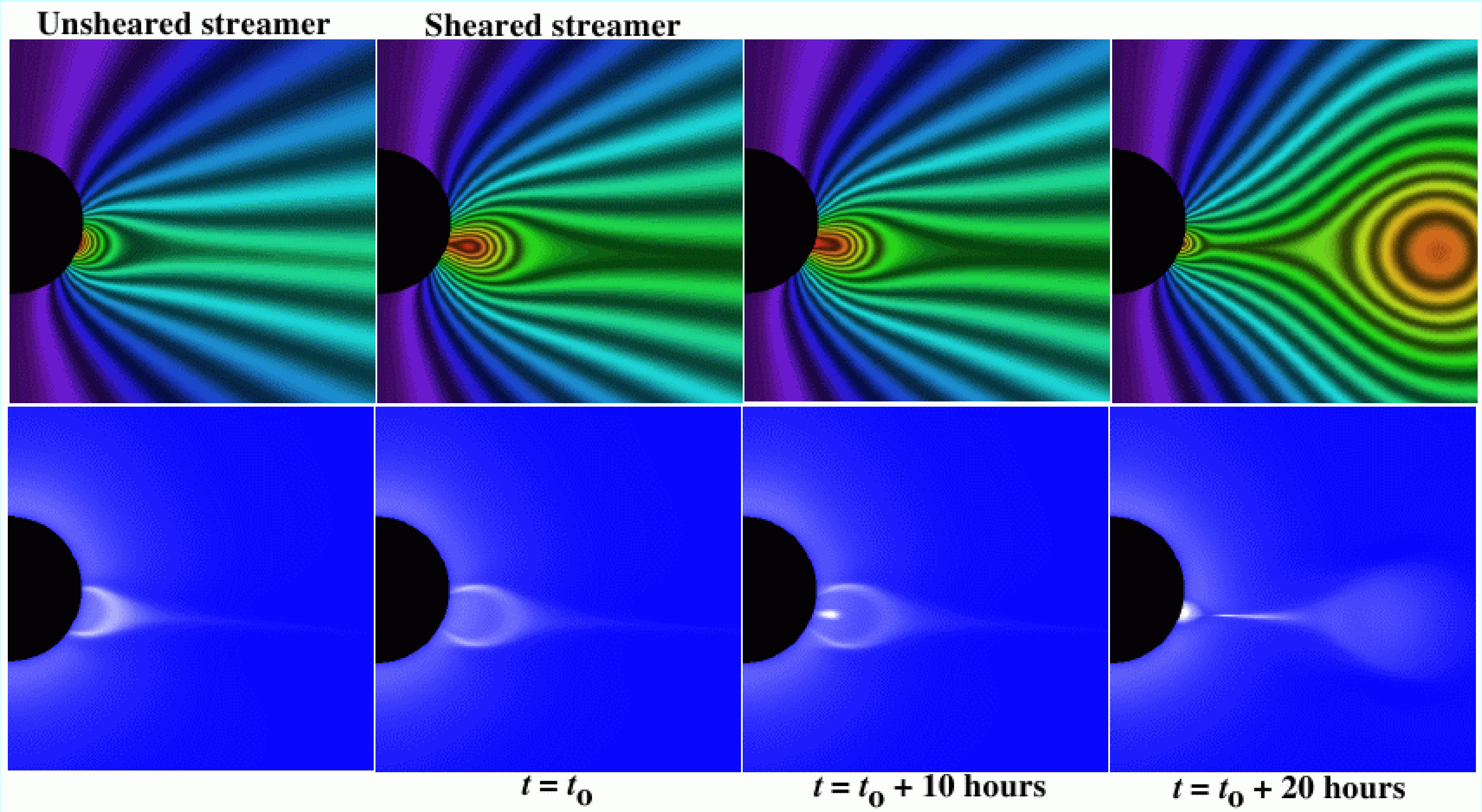

MAS/ENLIL code → streamer, eruption and evolution of CME (Mikic & Linker 1994; Lionello et al. 1998; Mikic et al. 1999) Linker et al. 1999)

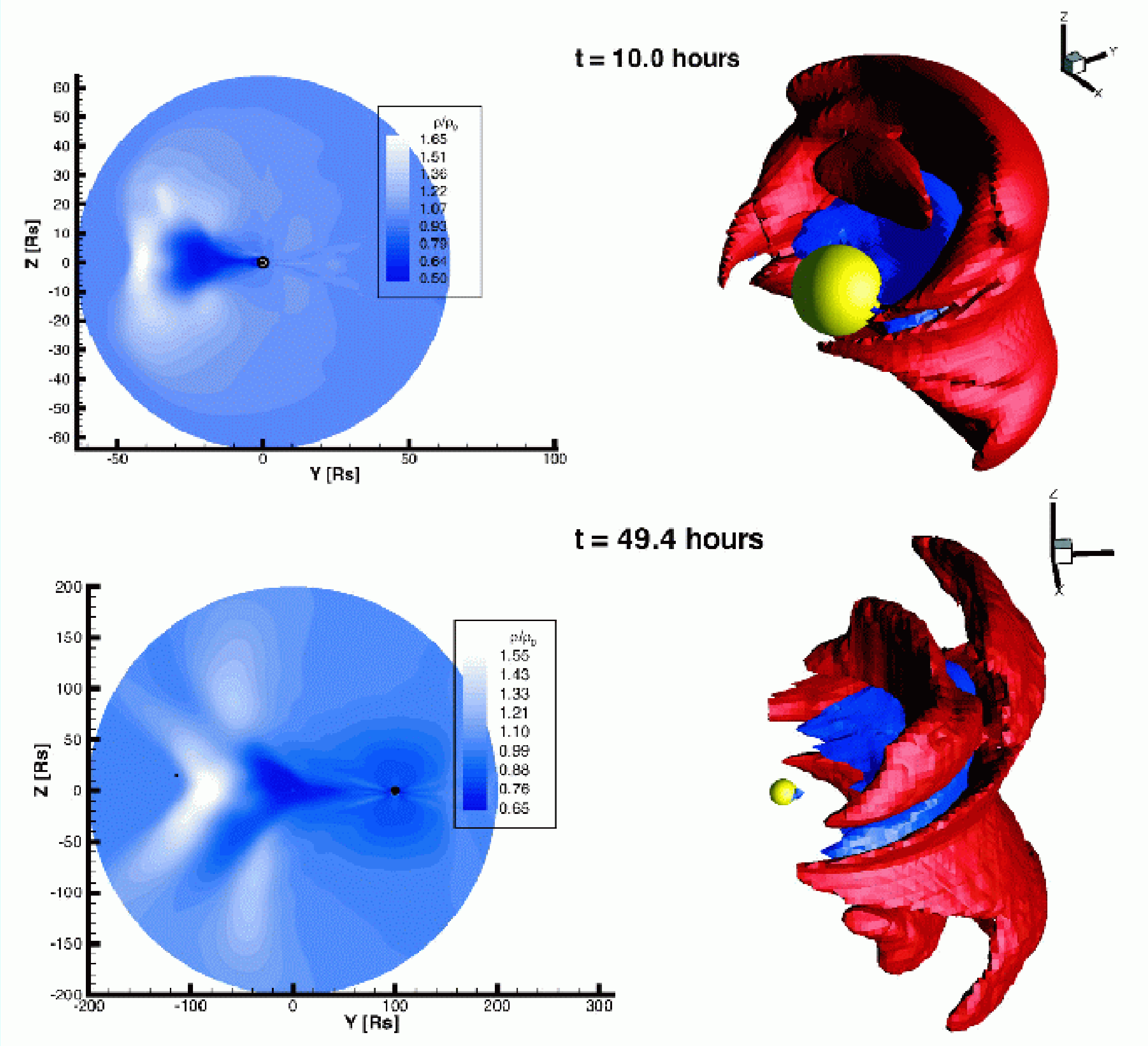

BATS`R'US-code (ideal MHD code)

Simulates launch of CME by loss of equilibrium of fluxrope (Roussev et al. 2004; Lugaz, Manchester & Gombosi 2005)

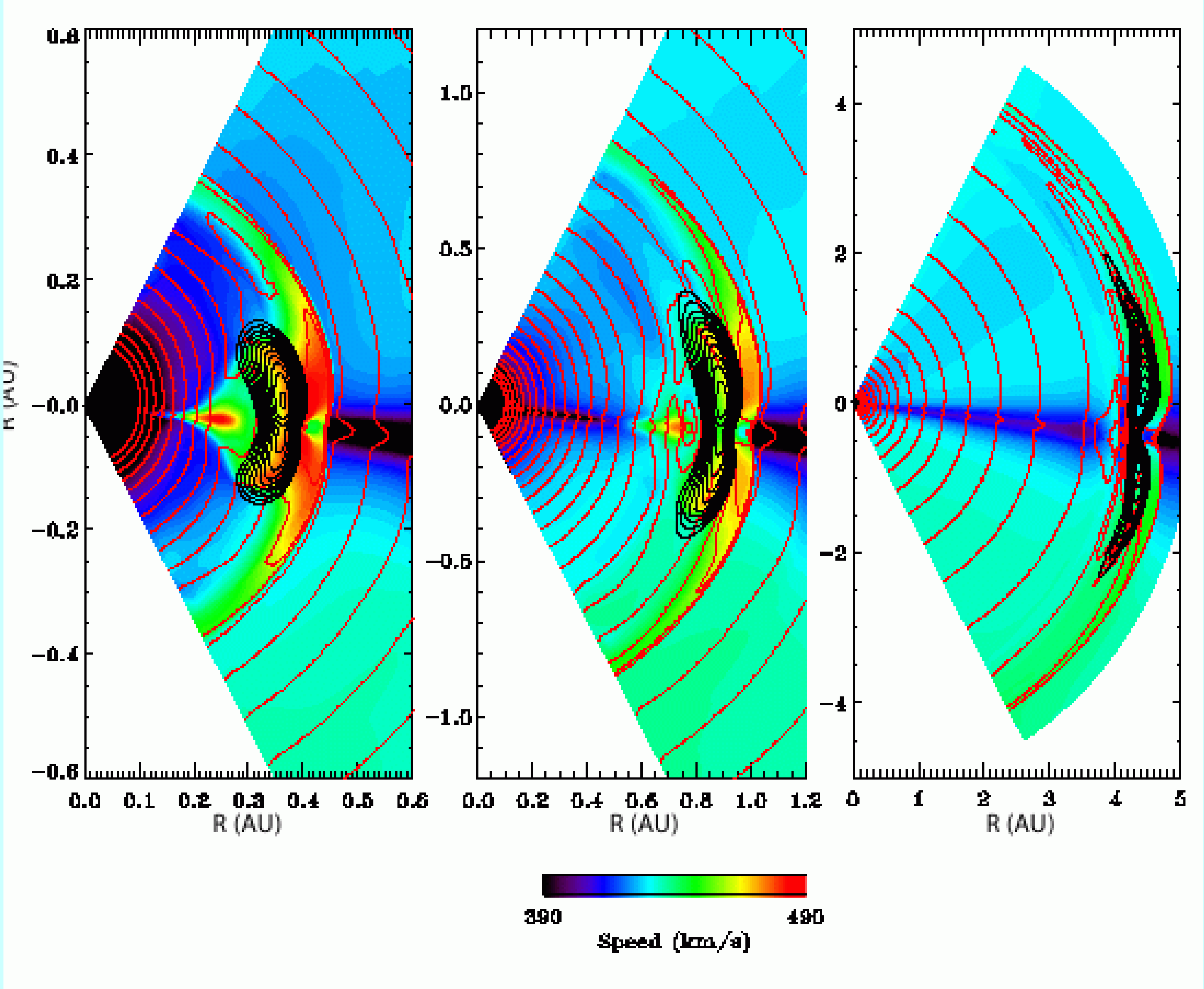

ENLIL+MAS code: simulates propagation of CME in solar wind, produces accurate shock strenghts, arrival of shocks at 1 AU (Odstrcil et al. 1996, 2002 2004, 2005; Odstrcil & Pizzo 1999)

Observation of CME Structure with LASCO/SoHO

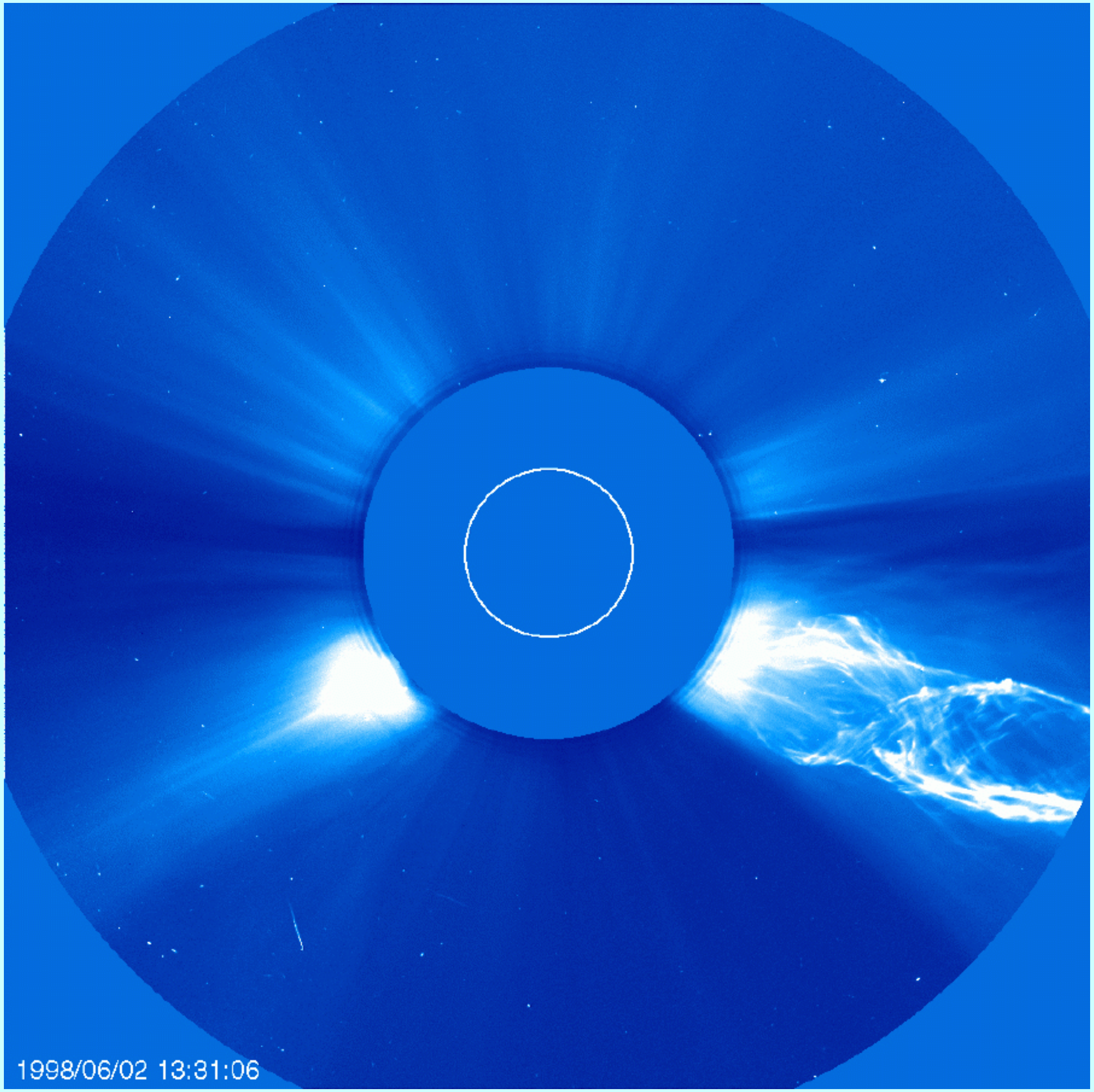

3D Reconstruction from 2 STEREO images

(either from EUVI or white-light coronagraphs)

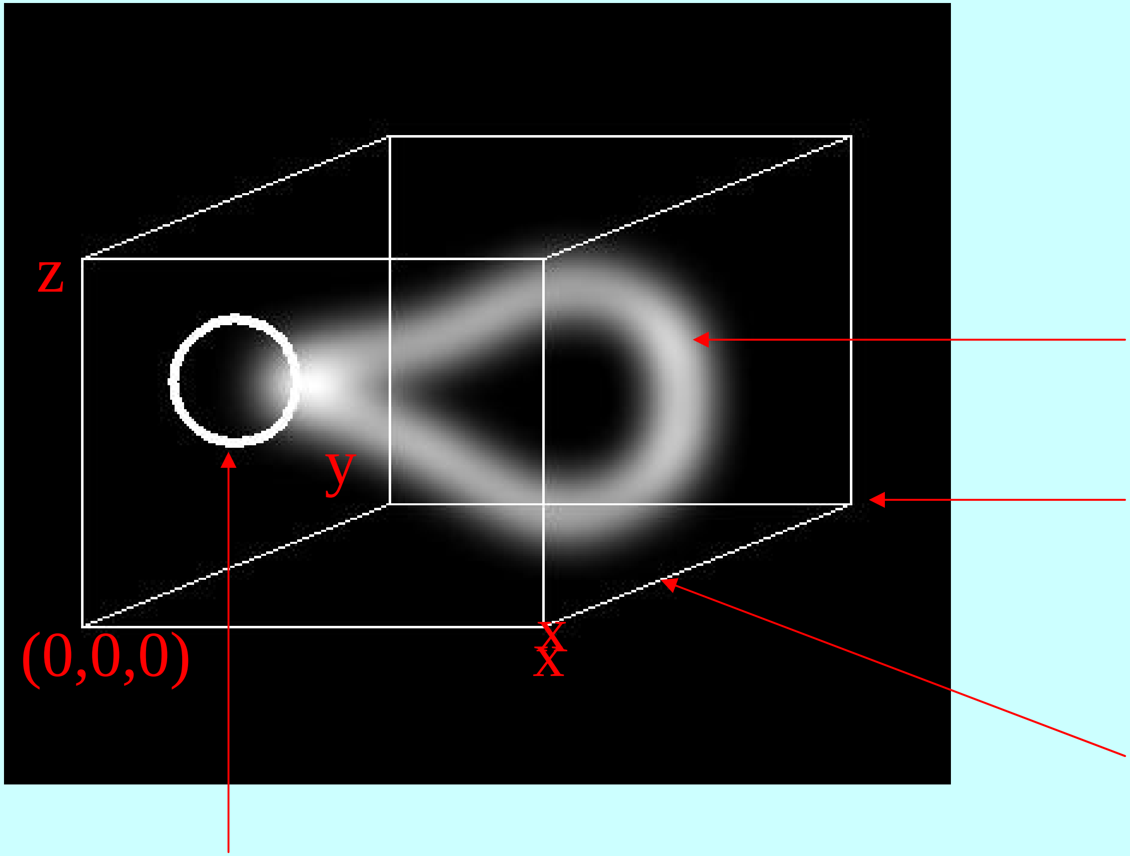

Slices with independent 2D reconstructions :

- Adjacent solutions can be used as additional constraints

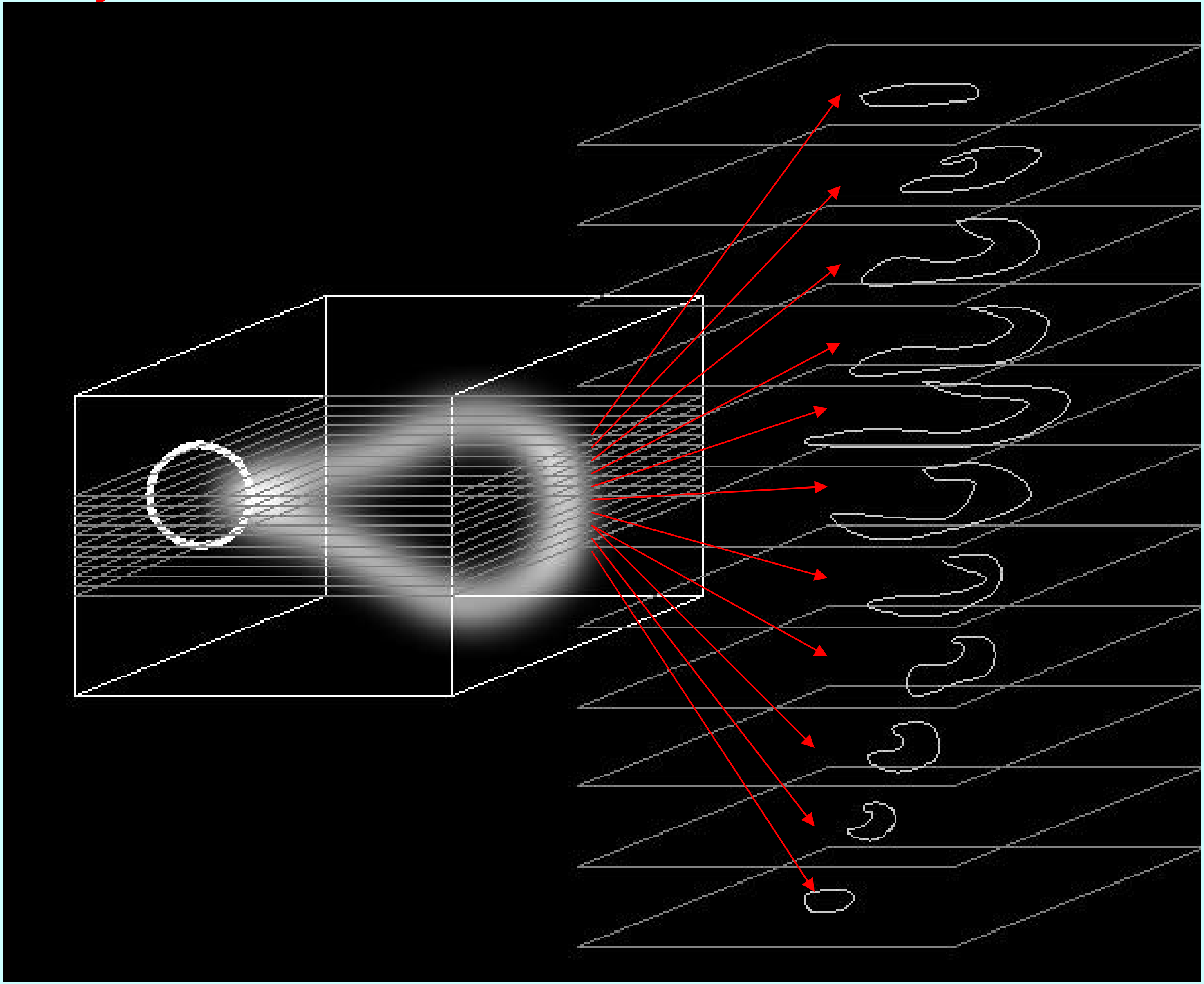

2D Slices of reconstruction from 2 views

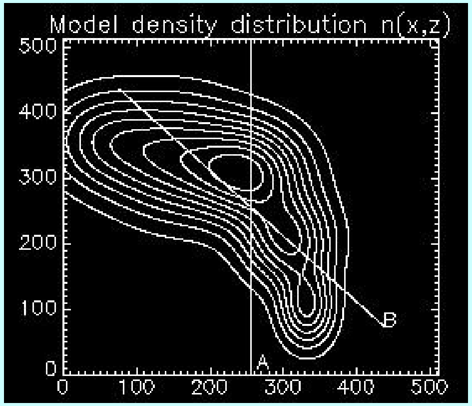

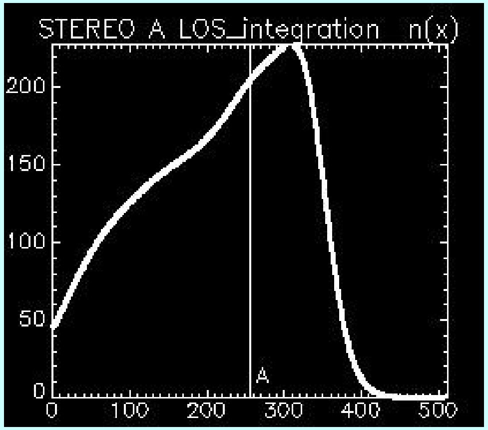

STEREO-A

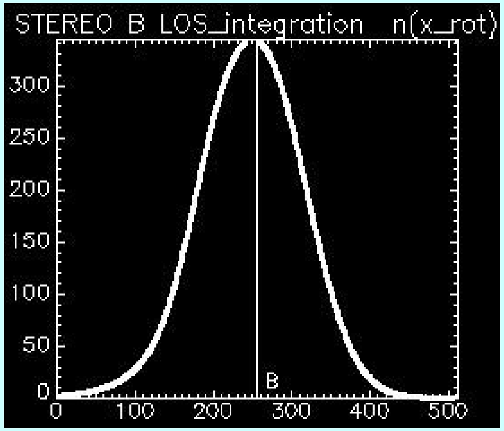

STEREO-B

Is 2D reconstruction from two projections unique ?

$$f(x,y)$$

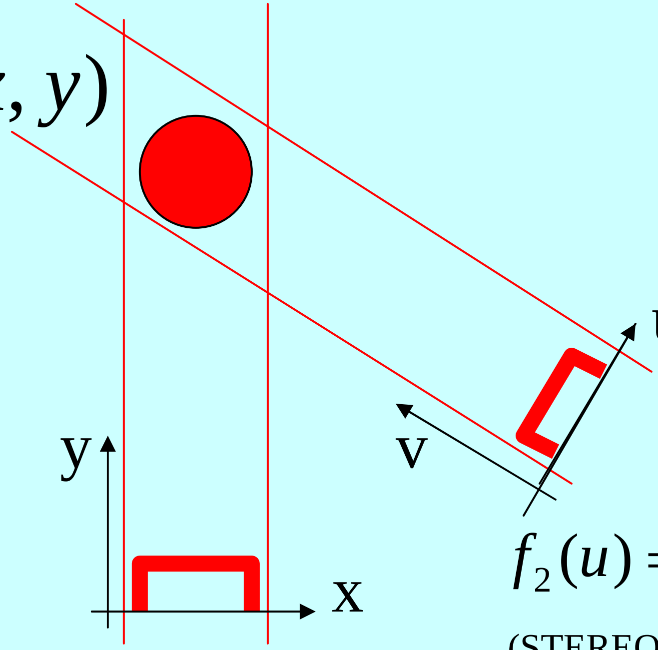

Coordinate rotation (x,y) → (u,v) :

$$\begin{pmatrix} u-u_0 \\ v-v_0 \end{pmatrix} = \begin{pmatrix} \cos(\alpha) & \sin(\alpha) \\ -\sin(\alpha) & \cos(\alpha) \end{pmatrix} \begin{pmatrix} x-x_0 \\ y-y_0 \end{pmatrix}$$

$$f_2(u) = \int f(u[x,y], v[x,y])\,dv$$

(STEREO-B)

$$f_1(x) = \int f(x,y)\,dy$$

(STEREO-A)

$$\left.\begin{aligned} f_1(x) &= \int f(x,y)\,dy \\ f_2(u) &= \int f(u[x,y], v[x,y])\,dv \end{aligned}\right\} \xrightarrow{\text{INVERSION}} f(x,y)$$

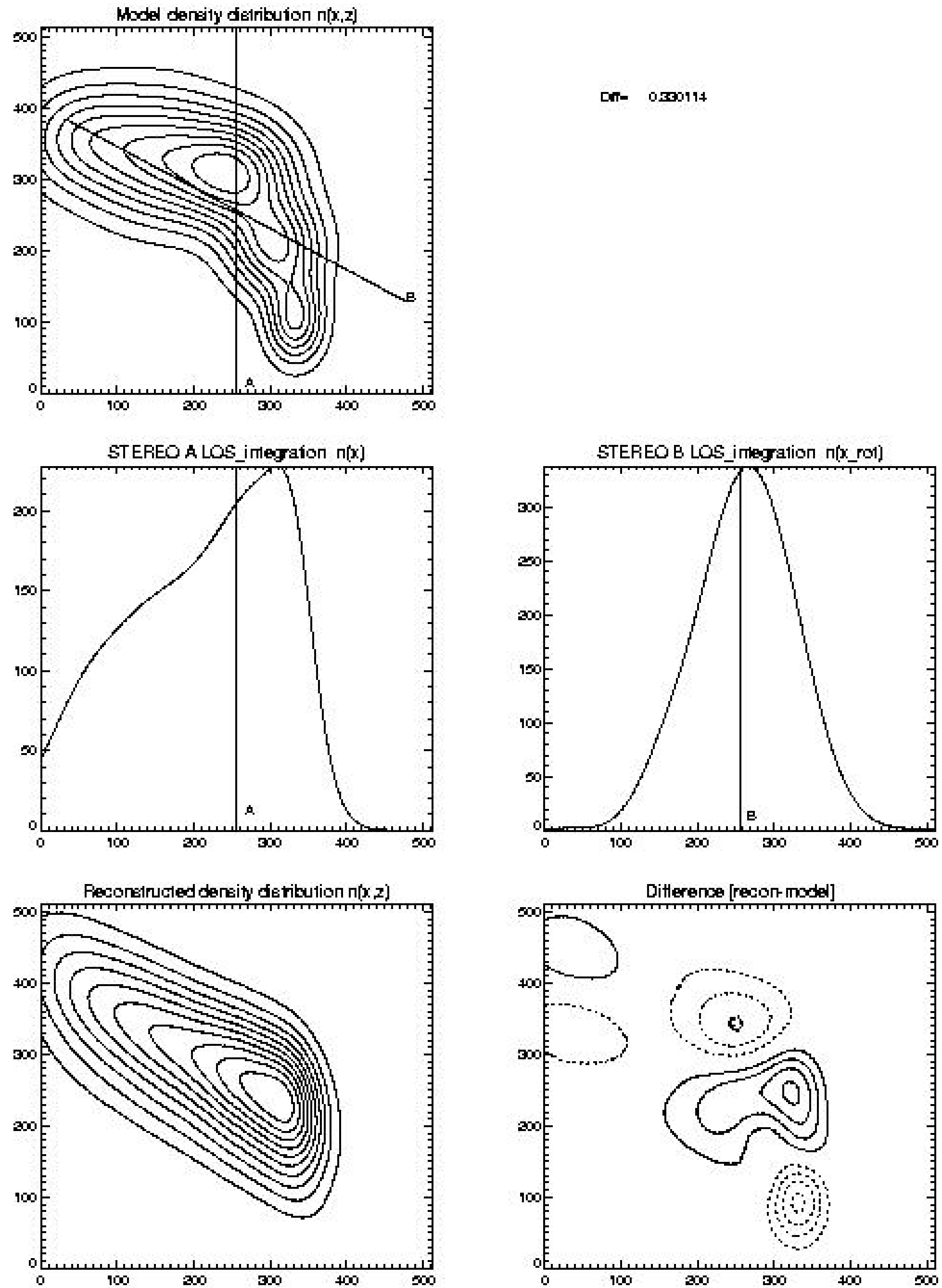
Model density distribution n(x,z)
Diff= 0.330114
STEREO A LOS_integration n(x)
STEREO B LOS_integration n(x_rot)
Reconstructed density distribution n(x,z)
Difference [recon-model]
A
B

6. Modeling of Interplanetary Shocks

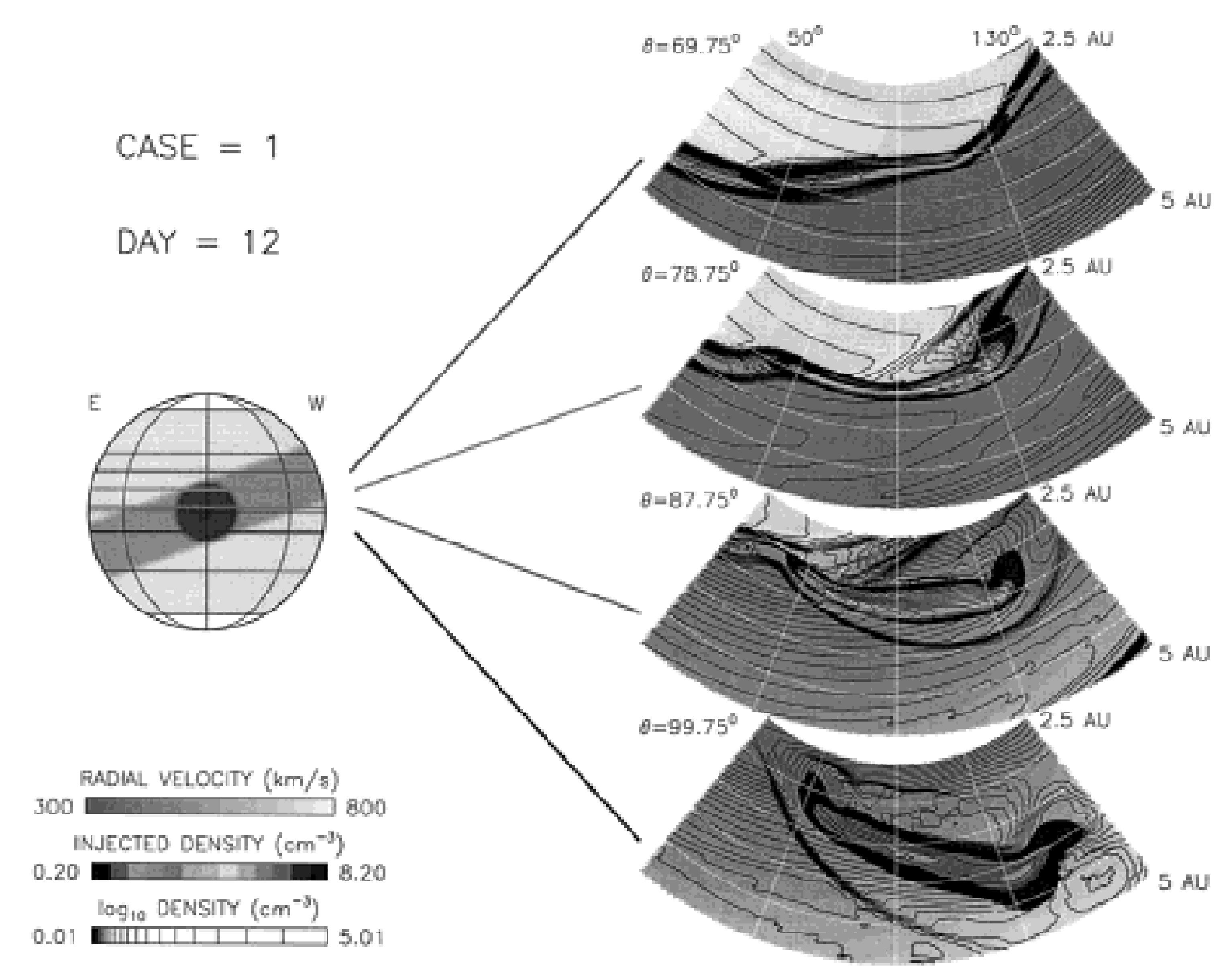

Odstrcil & Pizzo (1999)

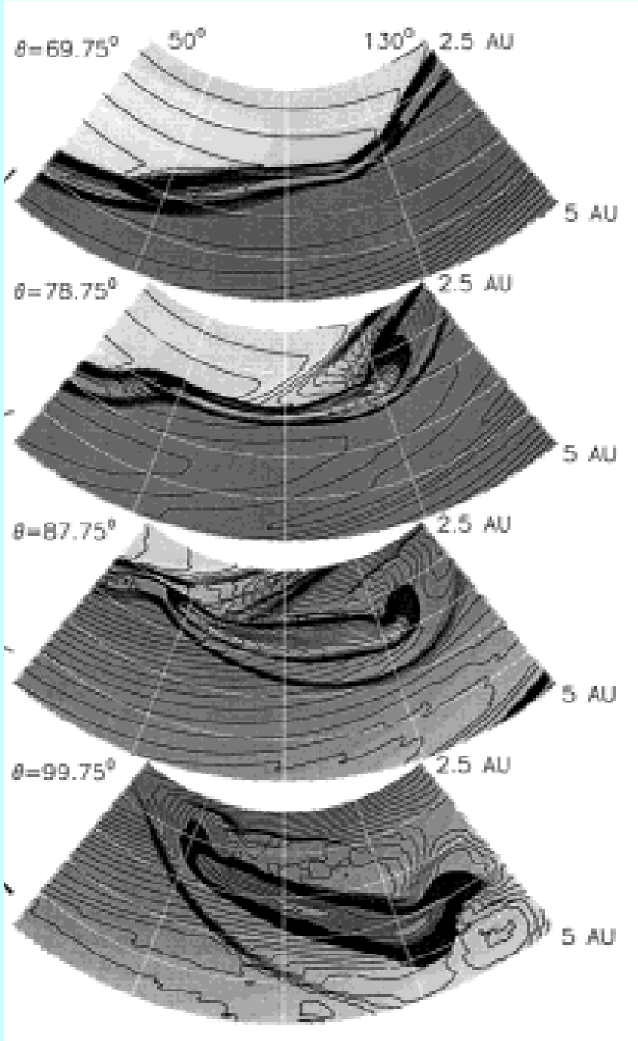

Odstrcil & Pizzo (1999)

Fast CMEs have speeds of v>2000 km/s
→formation of fast-mode shock
Numerical MHD simulations:

- Mikic & Linker (1994)
- Odstrcil & Pizzo (1999)
- Odstrcil, Pizzo, & Arge (2005)

Predicted arrival time at 1 AU depends critically on models of background solar wind which controls shock propagation speed

- Odstrcil, Pizzo & Arge (2005)

CME cannibalism (faster overtakes slower one) → compound streams, interactions with CIR (corotating interaction regions) → control shock-accelerated particles (SEPs)

7. Modeling of Interplanetary Particle Beams and Radio Emission

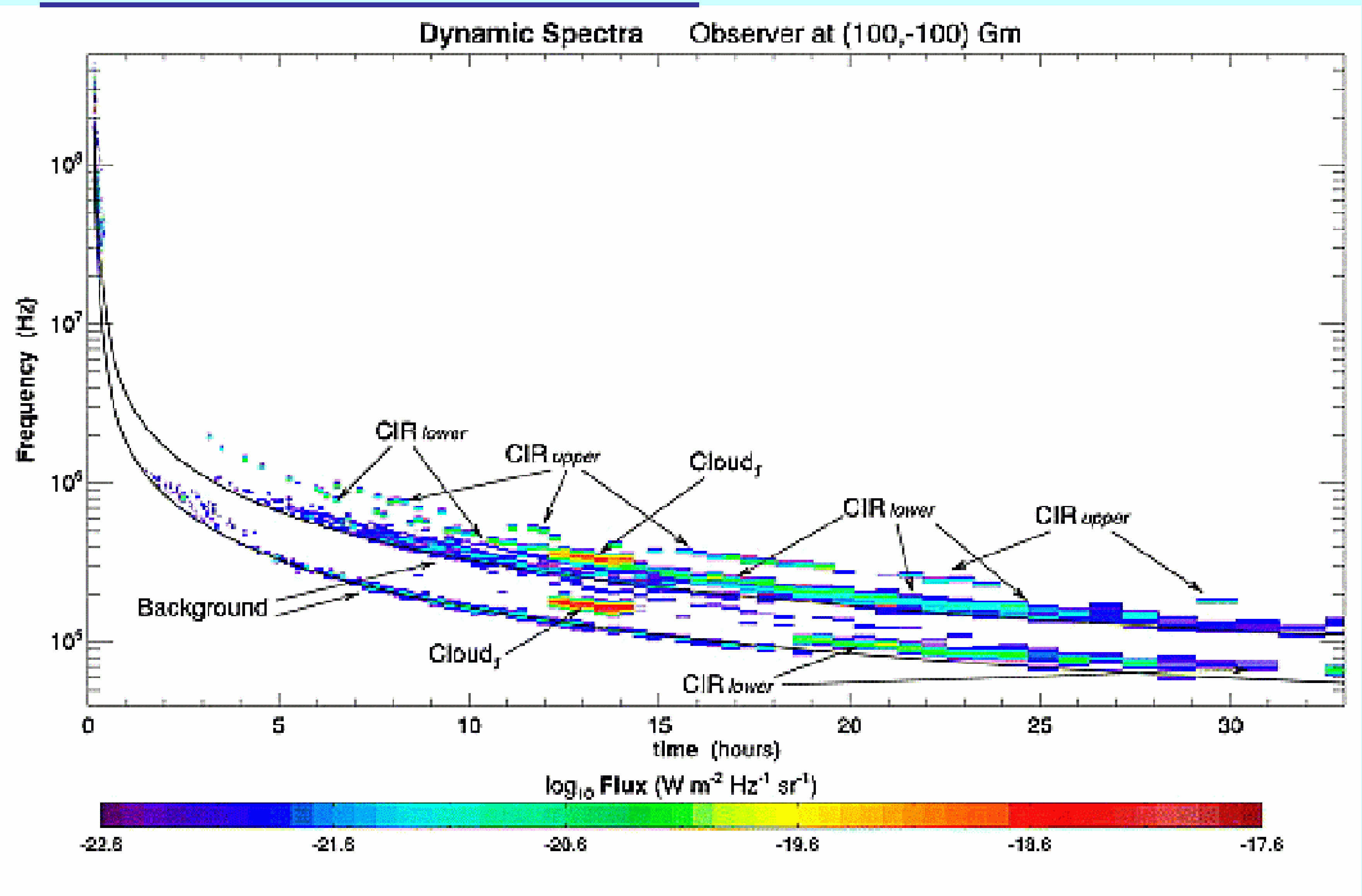

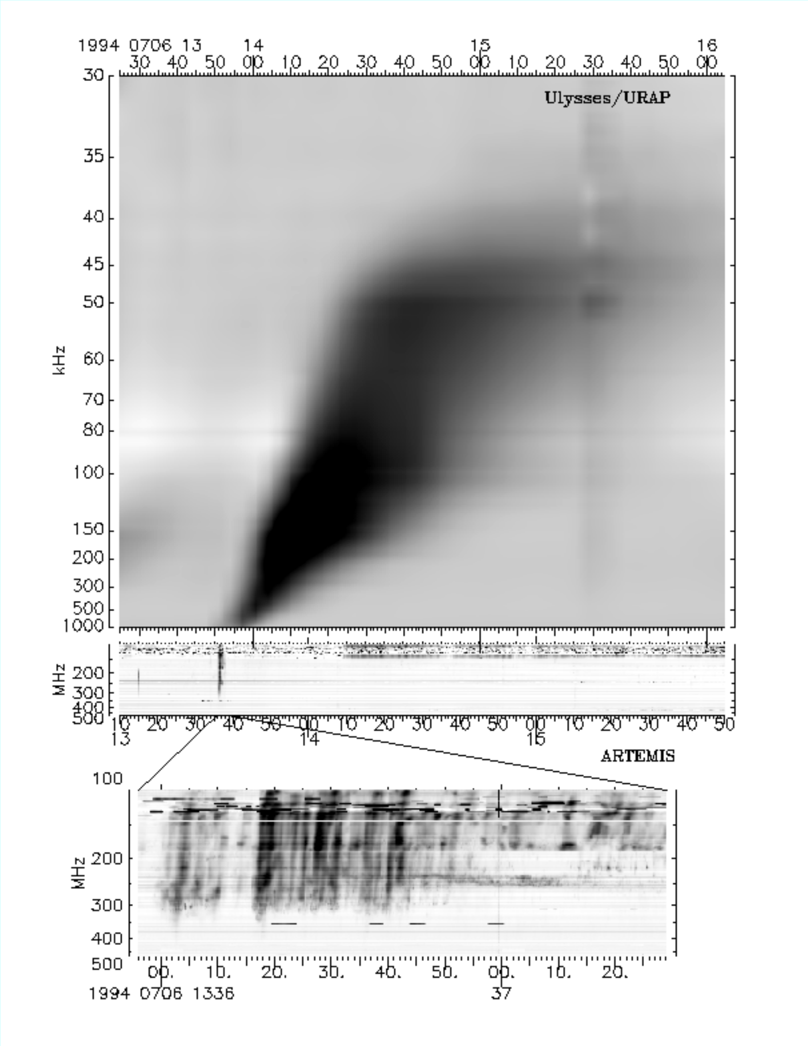

Pocquerusse et al. (1996)

Interplanetary radio emission

(see also talk by J-L. Bougeret)
-electron beams → type III
-shock waves → type II

IP space is collisionless
-propagation of suprathermal
 electron and ion beams

velocity dispersion
→bump-in-tail instability
→Langmuir wave growth at
 fundamental + harmonic
 plasma frequency (f_p~n_e^1/2)

stochastic growth theory
 Robinson & Cairns (1998)

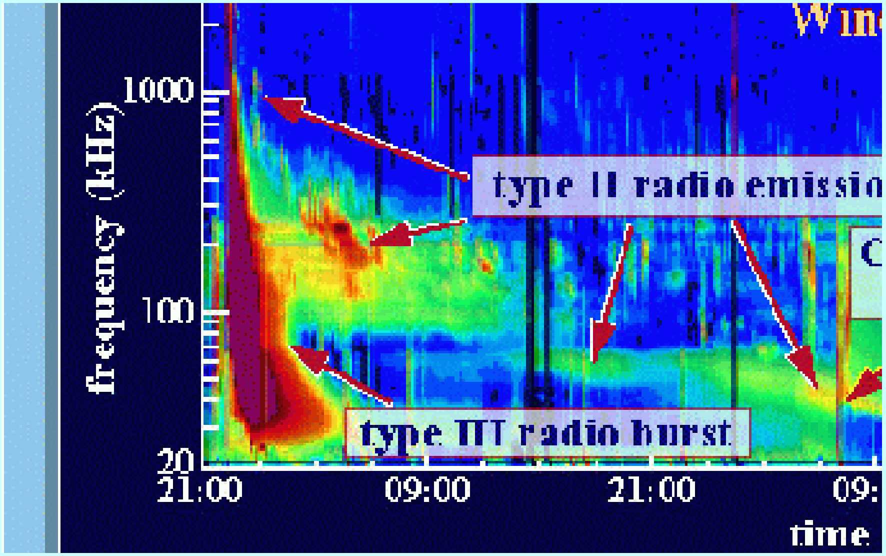

Type II bursts do not outline entire shock front, but occur only where shock wave intersects preexisting structures
Reiner & Kaiser (1999)

Interplanetary type II bursts were All found to be associated with fast CMEs, with shock transit Speeds v>500 km/s
Cane, Sheeley, & Howard (1987)

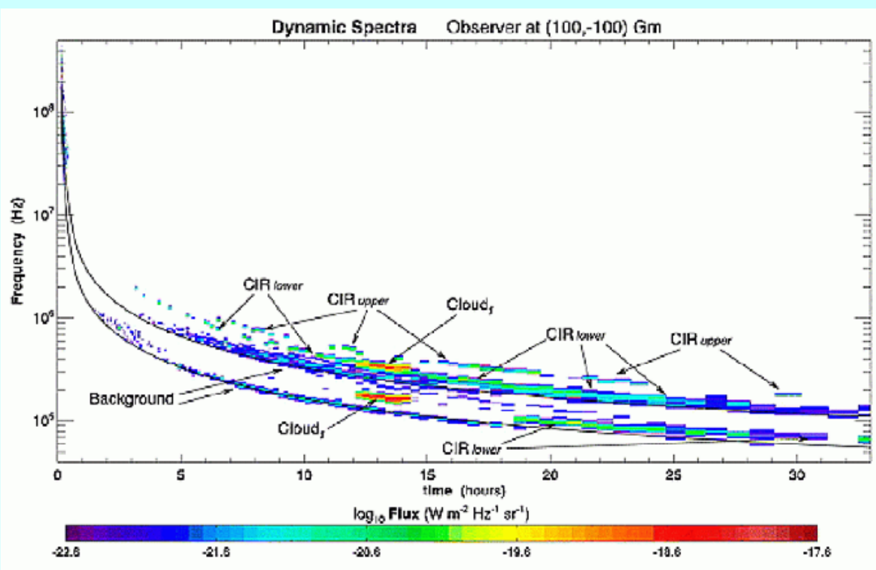

Semi-quantitative theory of type II bursts includes magnetic mirror reflection and acceleration of upstream electrons incident on shock (Knock & Cairns 2005)

In-situ particle + remote sensing (IMPACT + SWAVES)

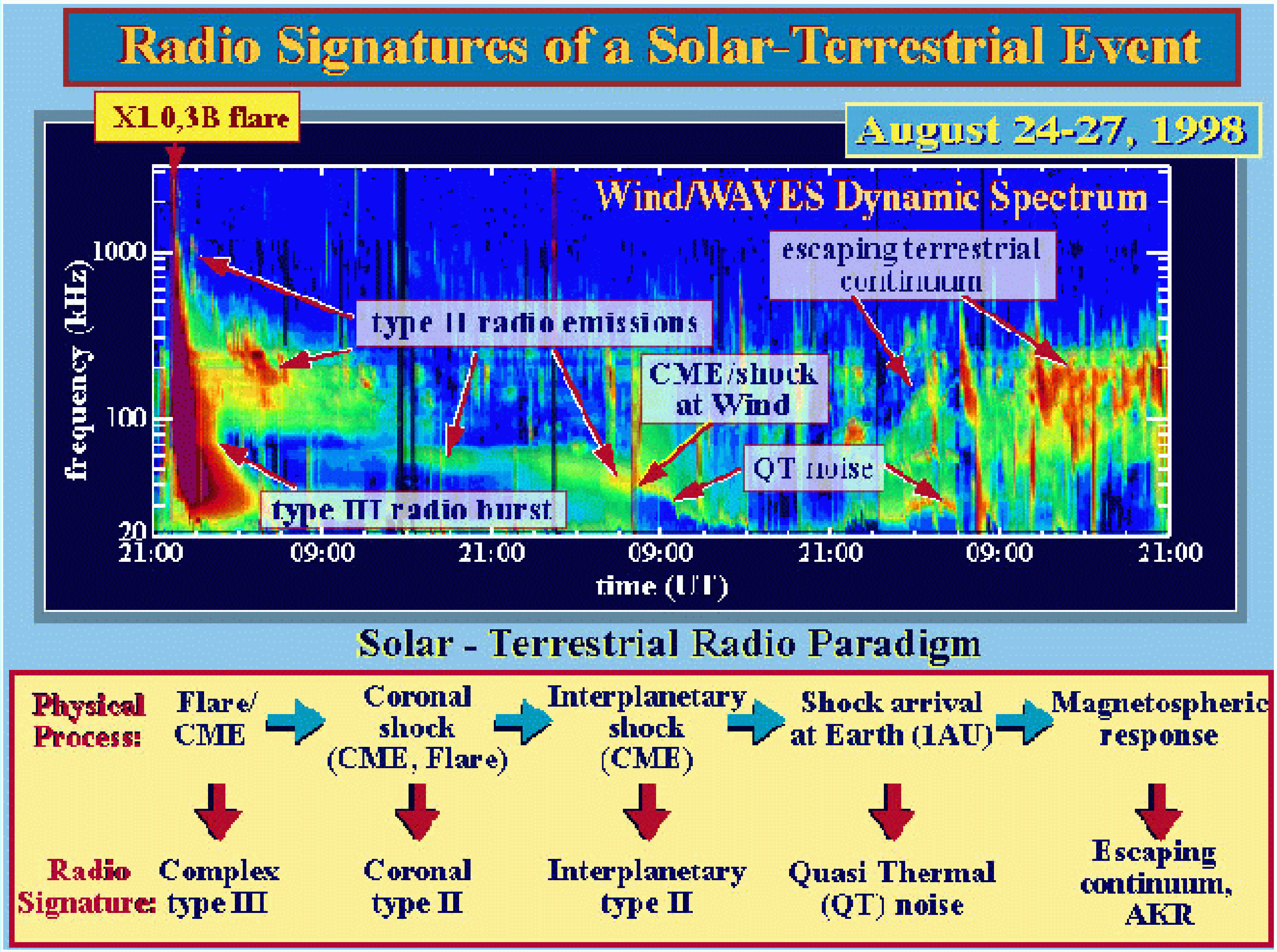

(courtesy of Mike Reiner)

8. Modeling of Solar Energetic Particles (SEPs)

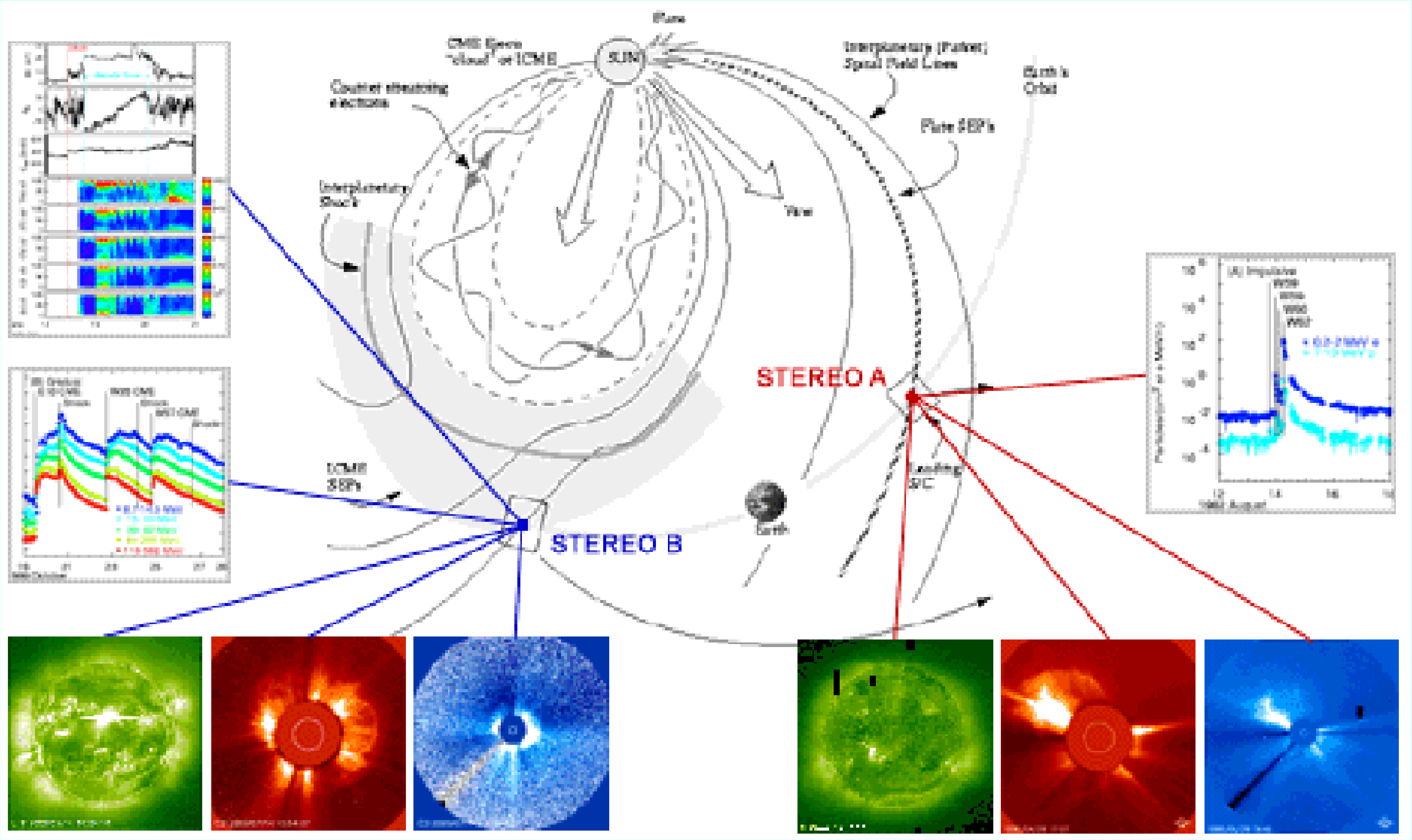

(see also talks by J.Luhmann and R.Mewaldt)

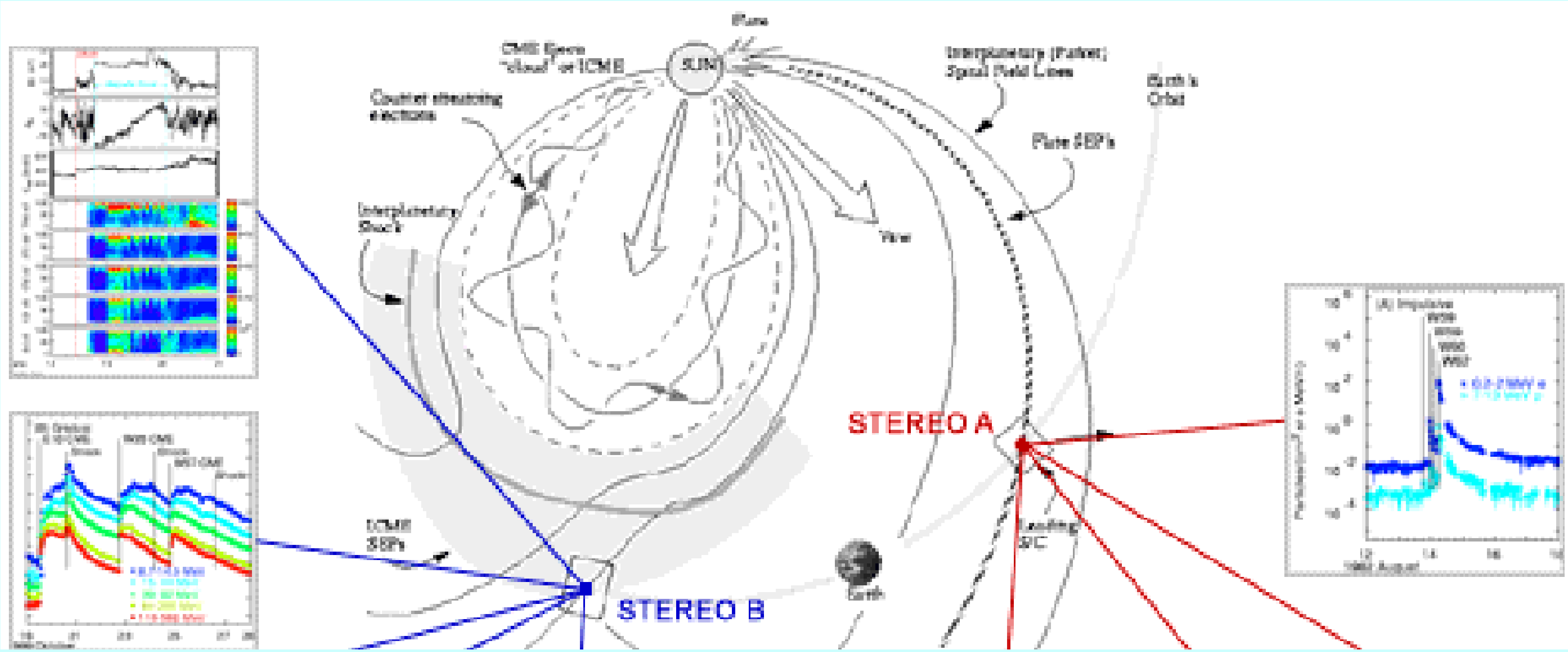

-Two-point in-situ measurements → acceleration of flare particles (A) versus acceleration in CME-driven shocks (B)

-Efficiency of quasi-parallel vs. quasi-perpendicular shock acc.

-Time-of-flight measurements at two spacecraft and Earth → localization of acceleration sources (flare, CME, CIR, CME front, preceding shock, CME flank, etc.)

-Quadrature observations → shock profile (A) and in-situ (B)

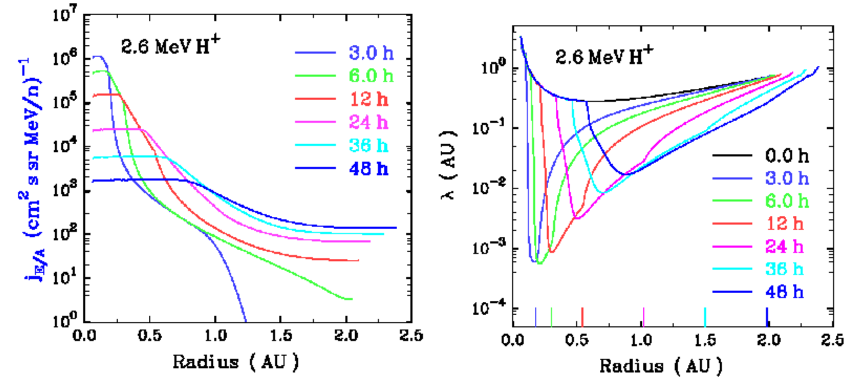

Figure 19. Coupled evolution of 2.6 MeV proton intensity (left) and mean free path (right) versus radius (Ng, Reames, & Tylka 2003).

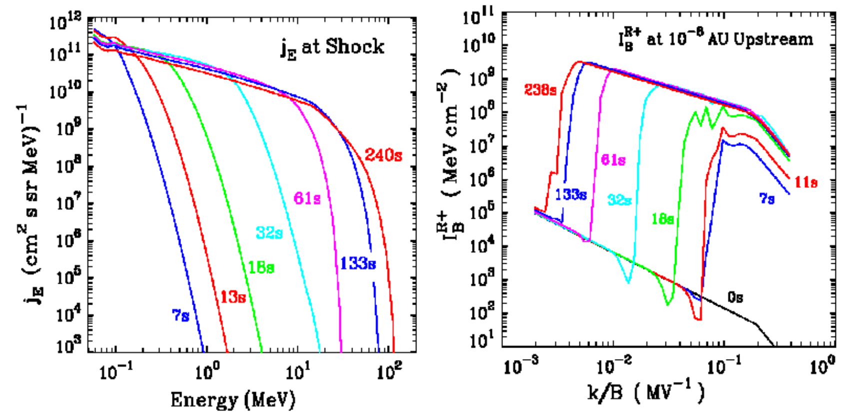

Figure 20. Proton acceleration (left) and Alfvèn wave growth (right) upstream of a moving shock at $\sim$ 3.7 solar radii (Courtesy of Chee Ng and Don Reames).

(Chee Ng & Don Reames)

Theoretical modeling of SEPs:

Diffusive shock acceleration, proton-excited Alfvenic waves upstream of shock, escape of particles upstream of the shock by magnetic focusing
(Marti Lee, 2005)

SEP propagation over several AU, fast acceleration by coronal shock, co-evolution of Alfven waves in inhomogeneous IP, focusing, convection, adiabatic deceleration, scattering by Alfven waves
→SEP fluxes and spectra
Modeling for STEREO/IMPACT
Tylka, Reames, & Ng (1999)

9. Modeling of Geo-effective events and Space Weather

-Arrival time of shocks at Earth will be improved by 3D triangulation of CME propagation with two spacecraft (STEREO →3D v-vector and r-vector reconstruction vs. LASCO →CME speed (lower limit) projected in plane of sky

-End-to-end models attempted including MHD of lower corona, heliosphere, and magnetosphere + SEP accel. & propagation

- CCMC (Community Coordinated Modelin Center, GSFC)
- CISM (Center for Integrated Space Weather Modeling, UCB)
- CSEM (Center for Space Environment Modeling, UMich)
- Solar/Muri (Solar Multidisciplinary Univ. Research Initiative)

CONCLUSIONS

-Theory and modeling efforts for the STEREO mission is designed for data data analysis of both remote-sensing (SECCHI, SWAVES) and in-situ instruments (IMPACT, PLASTIC).

-Modeling includes background plasma in corona, heliosphere, and solar wind, but concentrates on dynamic phenomena associated with initiation of CMEs in lower corona (filament dynamics, shearing, kinking, loss-of-equilibrium, filament eruption, magnetic reconnection in coronal flare sites), and propagation and evolution of CMEs in interplanetary space (interplanetary shocks, IP particle beams, SEP acceleration and propagation, geoeffective events, space weather), attempting end-to-end models from corona, trhough heliosphere, to magnetosphere).